Scientific report; 97 - 07

KNMI

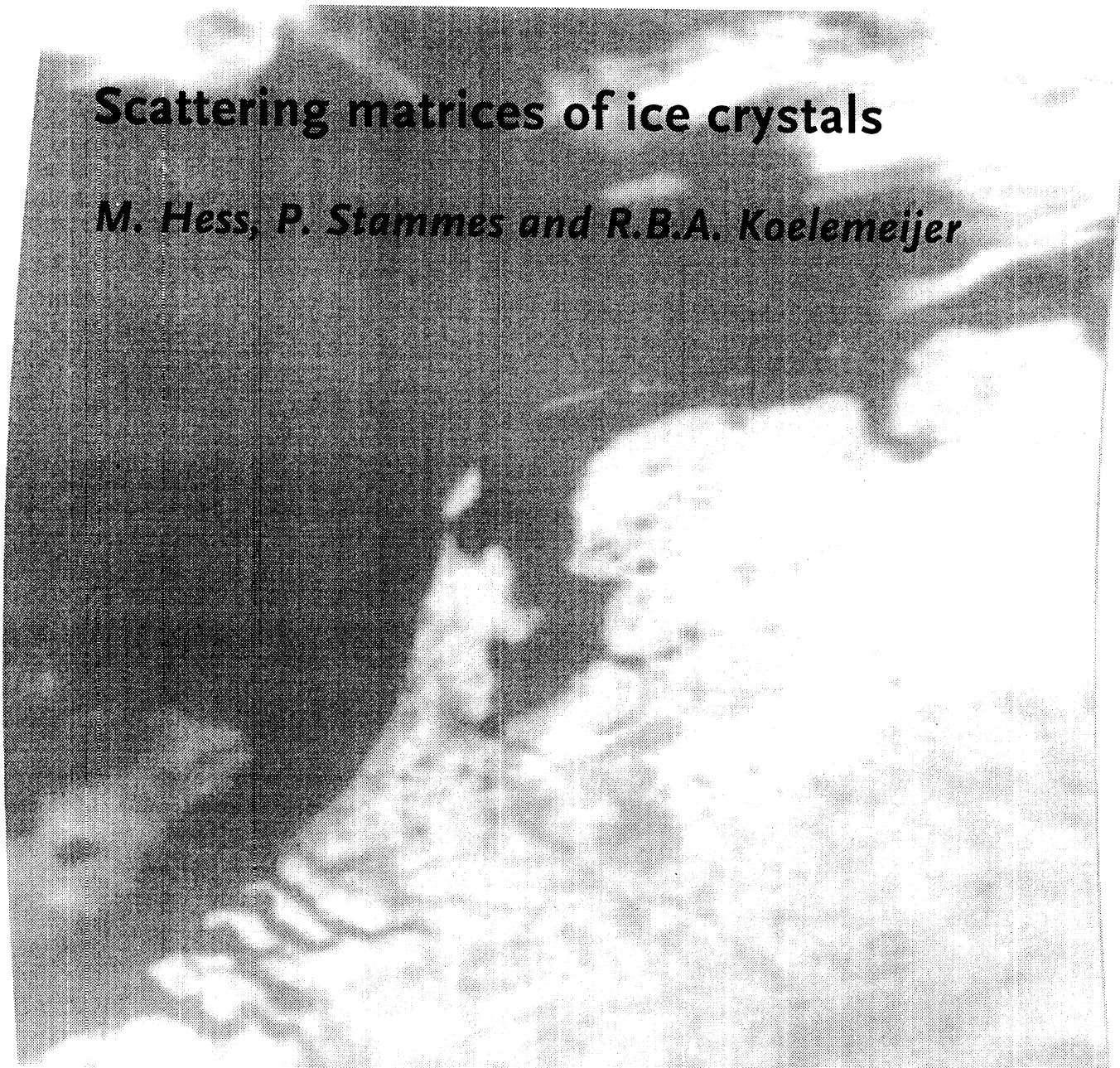

Scattering matrices of ice crystals

M. Hess, P. Stammes and R.B.A. Koelemeijer

De Bilt, 1997

Scientific report = wetenschappelijk rapport; WR 97 - 07

De Bilt, 1997

PO Box 201
3730 AE De Bilt
Wilhelminalaan 10
De Bilt
The Netherlands
Telephone + 31(0)30-220 69 11
Telefax + 31 (0)30-221 04 07

Authors: M. Hess, P. Stammes and
R.B.A. Koelemeijer

UDC: 551.521.3
551.578.41

ISSN: 0169-1651

ISBN: 90-369-2128-7

Scattering matrices of ice crystals

Michael Hess
Piet Stammes
Robert Koelemeijer

November 1997

Contents

Abstract

The present report describes the results of an eight months working visit of M.H. at KNMI. The goal of this visit was the implementation of cirrus clouds in the DAK radiative transfer model *(De Haan et al., 1987; Stammes, 1994))*. With this addition the DAK model can be used for the interpretation of satellite measurements of cirrus clouds.

The DAK radiative transfer model requires scattering matrices of atmospheric constituents which influence the radiation field in the atmosphere. The scattering matrices of ice crystals are calculated with help of a raytracing code using the geometric optics approximation, which is valid for particles considerably larger than the wavelength of the scattered radiation. An existing raytracing code for hexagonal columnar and platelike ice crystals *(Hess and Wiegner, 1994)* is extended to calculate the complete 4×4 scattering matrix containing the full polarisation information. It is also extended to allow calculations for spherical particles and for non-ideal hexagonal crystals. Scattering by non-ideal ice crystals is modelled by means of statistical variation of ray paths during the raytracing in regular hexagonal particles. A first application to radiative transfer calculations of cirrus clouds is shown.

1 Introduction

Scattering matrices of atmospheric particles are needed to calculate the radiation field in the atmosphere, which depends on the amount, size, shape, and chemical composition of the particles and on their height distribution in the atmosphere. Calculations of radiation fluxes or of radiances, at top and bottom of the atmosphere, are needed for the interpretation of all kinds of radiation measurements, especially for satellite measurements. Most of the atmospheric particles may be described as spheres, which allows the use of Mie theory for the calculation of their single scattering properties. However, Mie theory cannot be used to model non-spherical particles, like ice crystals in cirrus clouds. They have to be described using the hexagonal crystaline structure of ice. In the size range of several hundred microns this can up to now only be achieved with help of raytracing models, which are based on the geometric optics approximation.

The aim of this report is to provide single scattering matrices of hexagonal ice crystals, which can be used as input data for the DAK radiative transfer model. This is done by extending an existing raytracing code *(Hess and Wiegner, 1994)* with the complete polarisation calculation. The non-ideal shape of ice crystals is also taken into account by application of statistical variations of the ray paths during the raytracing in regular hexagonal crystals.

This report also serves as a description of the methods and algorithms which are used in the raytracing code. Therefore, the description is in some cases closer to the way in which the algorithms are coded, than to an elegant mathematical description. Only those parts of the raytracing code which have been changed during these months are described in the report. For further information the reader is referred to *Hess (1996)*.

2 Spherical particles

In order to have a model whose results are easier to understand and therefore easier to check than the model for hexagonal ice crystals, a special version of the raytracing code was made, which allows calculations for spheres. In this case the expected results are well known and the convergence is much faster because of the special geometry. Moreover, all interactions take place in the same plane, and therefore the effect of the rotation of the Stokes vectors can be excluded for the first tests. In the following sections, the changes in the description of the particle and raytracing geometry necessary for spheres are described and the diffraction formula for spheres is given.

2.1 Determination of point of incidence for incoming radiation

In Fig. 1, the geometry for raytracing in spheres is depicted. Because of the spherical symmetry only interactions that take place in one plane have to be considered, e.g. the plane of paper. Also, it is sufficient to consider incoming radiation incident from one direction and falling on one half of the circle. The direction of incidence is chosen to be the positive z-axis, the y-z plane is chosen as the scattering plane.

The number of rays falling on a certain part of the circle, here described by the radius in y-direction, is not equally distributed along the y-axis. It is proportional to the area of rings on the surface of the sphere, which have the same distance in the y-direction. This area is inversely proportional to the radius of these rings. This dependence is achieved in the following manner: a random number is chosen between zero and the particle radius. Then a second random number between zero and radius is chosen, which is used as point of incidence, if it is smaller than the first one. Otherwise it is refused and a new random number is chosen.

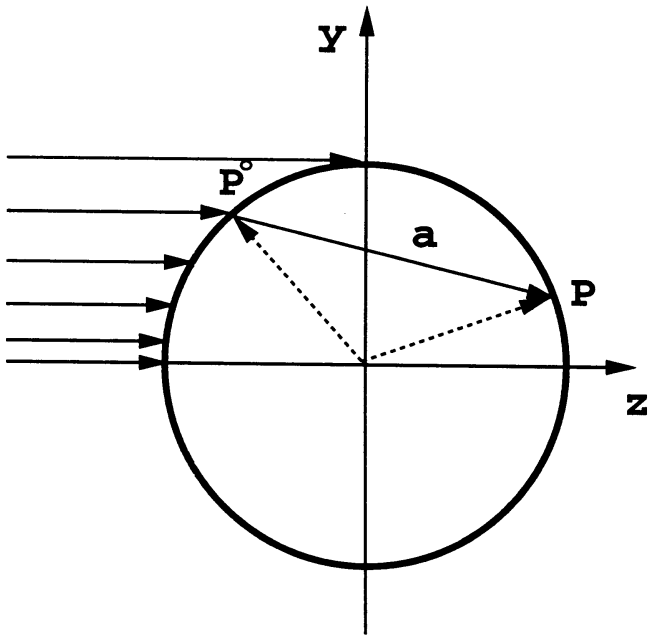

Figure 1: *Geometry of raytracing in a sphere with radius R. The y-z plane is the scattering plane, P_0 is the first point of incidence, P is the new point of interaction of the ray with the surface, and $\vec{a}$ is the vector describing the new direction of incidence at point P.*

2.2 Calculation of new ray direction after interaction with particle boundary

After each interaction with the boundary of the sphere, the new directions of the reflected and refracted rays have to be found. The geometry of this problem is depicted in Fig. 2. Because there is no dependence on the x-axis, the general set of equations is reduced to two equations, which can easily be solved. In the following, the equations for the refracted ray b_t are shown. Similar equations hold for the reflected ray b_r (cf. Sect. 4.1).

$$\begin{aligned} \vec{b_t} \cdot \vec{f_n} &= \cos(\theta_t) \\ \vec{b_t} \cdot \vec{a} &= \cos(\theta_d) = \cos(\theta_i - \theta_t) \end{aligned} \tag{1}$$

The solution is:

$$\begin{aligned} b_{t1} &= 0 \\ b_{t2} &= \frac{1}{a_2}(\cos(\theta_d) - a_3 b_3 \\ b_{t3} &= \frac{a_2 \cos(\theta_t) - f_{n2} \cos(\theta_d)}{a_2 f_{n3} - a_3 f_{n2}} \end{aligned} \tag{2}$$

or, if $a_2 = 0$:

$$\begin{aligned} b_{t1} &= 0 \\ b_{t2} &= \frac{1}{f_{n2}}(\cos(\theta_t) - b_3 f_{n3}) \\ b_{t3} &= \frac{1}{a_3} \cos(\theta_d) \end{aligned} \tag{3}$$

2.3 Calculation of new point of interaction with particle boundary

According to Fig. 1, the new point of intersection P of the ray with the surface may be calculated from the former one P_0, if the direction of the ray is known. The center of the sphere is chosen as the origin of the coordinate system. The coordinates of the points P_0 and P are related in the following way, where (y_s, z_s) is the (known) unit vector in the new ray direction, which has the unknown length a:

$$\begin{pmatrix} y_{p_0} \\ z_{p_0} \end{pmatrix} + a \begin{pmatrix} y_s \\ z_s \end{pmatrix} = \begin{pmatrix} y_p \\ z_p \end{pmatrix} \tag{4}$$

a is the length of the ray path between two intersections and is therefore also needed for calculating the absorption. The needed third condition is that the new intersectional point has to be part of the circle with radius R. Therefore, the third equation is

$$y_p^2 + z_p^2 = R^2 \tag{5}$$

This gives a quadratic equation with a solution for a, which only depends on the former intersection point (y_{p_0}, z_{p_0}) and the ray direction (y_s, z_s):

$$a = \frac{-2(y_s y_{p_0} + z_s z_{p_0}) \pm \sqrt{2(y_s y_{p_0} + z_s z_{p_0})^2 - 4 y_s^2 z_s^2 (y_{p_0}^2 + z_{p_0}^2 - R^2)}}{2 y_s^2 z_s^2} \tag{6}$$

Only one of the two possible solutions yields a positive result for a.

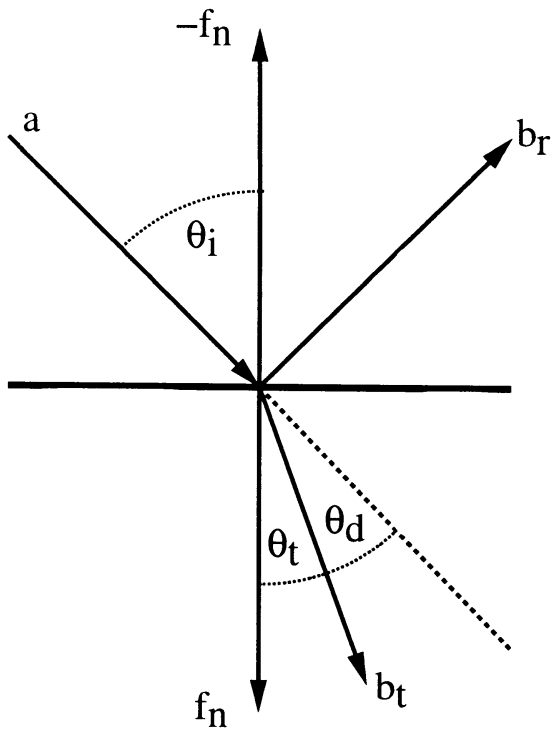

Figure 2: *Geometry for new ray directions.* θ_i *is the angle of incidence,* θ_t *the angle of refraction,* $\vec{a}$ *is the direction of the incoming ray,* $\vec{f}$ *is the plane normal,* $\vec{b_t}$ *is the direction of the refracted ray, and* $\vec{b_r}$ *is the direction of the reflected ray.*

2.4 Diffraction for spheres

The diffraction function for a sphere with radius R and the wavelength λ is given by:

$$d(\theta) = \frac{x^4}{4}(1 + \cos(\theta)) \left[\frac{J_1(x \sin(\theta)}{(x \sin(\theta)}\right]^2 \tag{7}$$

with the *Bessel function* J_1 and the size parameter

$$x = \frac{2\pi R}{\lambda} \tag{8}$$

To get rid of the oscillations showing up in calculations for a single sphere, the diffraction is averaged over a size distribution:

$$n(r) = n_o r^6 e^{(-9r/R)} \tag{9}$$

This distribution has been proposed by *Deirmendjian (1969)* and often been used in the literature for this purpose. The diffraction is calculated for 100 radii with steps of 1 in size parameter around the radius R. The resulting diffraction function is normalized to unity.

3 Scattering matrix

This chapter describes the main purpose of the current work. The raytracing code is extended in such a way that the calculation of the 4×4 scattering matrix becomes possible. The existing code already calculated the state of polarisation of the scattered radiation, i.e. its Stokes vector. This means that the calculated polarisation of the scattered radiation was dependent on the Stokes vector of the incident radiation. In the matrix description, all possible cases of incident polarisation are included.

Intensity and polarisation of radiation are completely described by the Stokes vector $(I_\perp, I_\parallel, U, V)$. $I_\perp$ and $I_\parallel$ are the intensities perpendicular and parallel to a certain plane of reference, which contains the direction of propagation. Each change of the Stokes vector may be expressed by a 4×4 matrix. In case of a scattering process, the matrix $\mathbf{F}$ is the scattering matrix:

$$\begin{pmatrix} I_\perp \\ I_\parallel \\ U \\ V \end{pmatrix} = \begin{pmatrix} F_{11} & F_{12} & F_{13} & F_{14} \\ F_{21} & F_{22} & F_{23} & F_{24} \\ F_{31} & F_{32} & F_{33} & F_{34} \\ F_{41} & F_{42} & F_{43} & F_{44} \end{pmatrix} \begin{pmatrix} I_\perp^o \\ I_\parallel^o \\ U^o \\ V^o \end{pmatrix} = \mathbf{F}(\theta, \phi) \begin{pmatrix} I_\perp^o \\ I_\parallel^o \\ U^o \\ V^o \end{pmatrix} \tag{10}$$

This matrix depends on the scattering angle θ and the scattering azimuth angle ϕ. The elements of this matrix obey certain internal relations which can be used for testing the matrix (cf. chapter 8). If the scattering particles are randomly oriented in space, this matrix consists of only 6 independent non-zero elements, which only depend on the scattering angle θ:

$$\begin{pmatrix} I_\perp \\ I_\parallel \\ U \\ V \end{pmatrix} = \begin{pmatrix} F_{11} & F_{12} & 0 & 0 \\ F_{12} & F_{22} & 0 & 0 \\ 0 & 0 & F_{33} & F_{34} \\ 0 & 0 & -F_{34} & F_{44} \end{pmatrix} \begin{pmatrix} I_\perp^o \\ I_\parallel^o \\ U^o \\ V^o \end{pmatrix} = \mathbf{F}(\theta) \begin{pmatrix} I_\perp^o \\ I_\parallel^o \\ U^o \\ V^o \end{pmatrix} \tag{11}$$

This case will be treated throughout this report.

3.1 The algorithm

In this section the calculation of the scattering matrix is described. The matrix calculations have first been included in the program version for spherical particles, and were later implemented in the ice crystal code when they had been checked sufficiently.

The principal method is the following. All changes that occur to the Stokes vector of a ray on its way through the particle are expressed in terms of a matrix of change, and all these matrices are multiplied to yield finally the scattering matrix. Changes to the Stokes vector occur:

1. at any intersection of a ray with the particle boundary, where the ray changes its direction and intensity according to the Fresnel formulae
2. because of the rotation of the plane of reference of the Stokes vector into a new plane of incidence or into the scattering plane
3. because of absorption
4. due to diffraction.

Fresnel matrix

Throughout the raytracing code, the Stokes vector is used in the form $(I_\perp, I_\parallel, U, V)^\top$. In this notation, and assuming that changes in one of the two intensity components are not influenced by the other

one, a transformation matrix of the following form is valid according to *v.d. Hulst (1957)*, page 45:

$$\begin{pmatrix} I_\perp \\ I_\parallel \\ U \\ V \end{pmatrix} = \begin{pmatrix} a_1 & 0 & 0 & 0 \\ 0 & b_2 & 0 & 0 \\ 0 & 0 & \sqrt{a_1 b_2}\cos(\delta) & -\sqrt{a_1 b_2}\sin(\delta) \\ 0 & 0 & \sqrt{a_1 b_2}\sin(\delta) & \sqrt{a_1 b_2}\cos(\delta) \end{pmatrix} \begin{pmatrix} I_\perp^o \\ I_\parallel^o \\ U^o \\ V^o \end{pmatrix} = \mathbf{G} \begin{pmatrix} I_\perp^o \\ I_\parallel^o \\ U^o \\ V^o \end{pmatrix} \tag{12}$$

This form is valid for the reflected and refracted rays, and in these cases, a_1 and b_2 are the Fresnel refraction or reflection coefficients for the two intensity components, respectively, and δ is the phase change between the two amplitudes due to refraction or reflection.

Rotation matrix

The rotation of the Stokes vector is described by the following matrix *(Coulson, 1988)*:

$$\begin{pmatrix} I_\perp \\ I_\parallel \\ U \\ V \end{pmatrix} = \begin{pmatrix} \cos^2(\gamma) & \sin^2(\gamma) & \frac{1}{2}\sin^2(2\gamma) & 0 \\ \sin^2(\gamma) & \cos^2(\gamma) & -\frac{1}{2}\sin^2(2\gamma) & 0 \\ -\sin(2\gamma) & \sin(2\gamma) & \cos(2\gamma) & 0 \\ 0 & 0 & 0 & 1 \end{pmatrix} \begin{pmatrix} I_\perp^o \\ I_\parallel^o \\ U^o \\ V^o \end{pmatrix} = \mathbf{R} \begin{pmatrix} I_\perp^o \\ I_\parallel^o \\ U^o \\ V^o \end{pmatrix} \tag{13}$$

where γ is the angle of rotation between the two reference planes in clockwise direction.

Absorption matrix

Absorption diminishes the Stokes vector by a certain factor, i.e. the Stokes vector is multiplied by a constant A. In matrix notation we have:

$$\begin{pmatrix} I_\perp \\ I_\parallel \\ U \\ V \end{pmatrix} = \begin{pmatrix} A & 0 & 0 & 0 \\ 0 & A & 0 & 0 \\ 0 & 0 & A & 0 \\ 0 & 0 & 0 & A \end{pmatrix} \begin{pmatrix} I_\perp^o \\ I_\parallel^o \\ U^o \\ V^o \end{pmatrix} = \mathbf{A} \begin{pmatrix} I_\perp^o \\ I_\parallel^o \\ U^o \\ V^o \end{pmatrix} \tag{14}$$

Raytracing scattering matrix

All the matrices mentioned so far are valid with respect to the actual reference plane of the Stokes vector. The raytracing scattering matrix is then calculated by multiplying the appropriate transformation matrices as they occur on the ray's path through the particle. When the reference plane changes, the rotation matrix is applied. As an example, the path of a ray which leaves the crystal after one internal reflection is traced. $\mathbf{I}^x$ is the Stokes vector belonging to the ray after x transformations:

1. Rotate from scattering plane to first plane of incidence. Since the scattering plane is not known in the beginning, this first rotation is actually the last matrix multiplication performed.
   $\mathbf{I}^1 = \mathbf{R}^1\mathbf{I}^0$

2. Apply Fresnel matrix for transmission:
   $\mathbf{I}^2 = \mathbf{G_t}^2\mathbf{I}^1 = \mathbf{G_t}^2\mathbf{R}^1\,\mathbf{I}^0$

3. Absorption on the way to the next point of intersection:
   $\mathbf{I}^3 = \mathbf{A}^3\mathbf{I}^2 = \mathbf{A}^3\mathbf{G_t}^2\mathbf{R}^1\,\mathbf{I}^0$

4. Rotate to next plane of incidence:
   $\mathbf{I}^4 = \mathbf{R}^4\mathbf{I}^3 = \mathbf{R}^4\mathbf{A}^3\mathbf{G_t}^2\mathbf{R}^1\,\mathbf{I}^0$

5. Apply Fresnel matrix for reflection:
   $\mathbf{I}^5 = \mathbf{G_r}^5\mathbf{I}^4 = \mathbf{G_r}^5\mathbf{R}^4\mathbf{A}^3\mathbf{G_t}^2\mathbf{R}^1\,\mathbf{I}^0$

6. Absorption on the way to the next point of intersection:
   $\mathbf{I}^6 = \mathbf{A}^6\mathbf{I}^5 = \mathbf{A}^6\mathbf{G_r}^5\mathbf{R}^4\mathbf{A}^3\mathbf{G_t}^2\mathbf{R}^1\,\mathbf{I}^0$

7. Rotate to next plane of incidence:
   $\mathbf{I}^7 = \mathbf{R}^7\mathbf{I}^6 = \mathbf{R}^7\mathbf{A}^6\mathbf{G_r}^5\mathbf{R}^4\mathbf{A}^3\mathbf{G_t}^2\mathbf{R}^1\,\mathbf{I}^0$

8. Apply Fresnel matrix for transmission:
   $\mathbf{I}^8 = \mathbf{G_t}^8\mathbf{I}^7 = \mathbf{G_t}^8\mathbf{R}^7\mathbf{A}^6\mathbf{G_r}^5\mathbf{R}^4\mathbf{A}^3\mathbf{G_t}^2\mathbf{R}^1\,\mathbf{I}^0$

9. Rotate to scattering plane:
   $\mathbf{I}^9 = \mathbf{R}^9\mathbf{I}^8 = \mathbf{R}^9\mathbf{G_t}^8\mathbf{R}^7\mathbf{A}^6\mathbf{G_r}^5\mathbf{R}^4\mathbf{A}^3\mathbf{G_t}^2\mathbf{R}^1\,\mathbf{I}^0$

Now, $\mathbf{R}^9\mathbf{G_t}^8\mathbf{R}^7\mathbf{A}^6\mathbf{G_r}^5\mathbf{R}^4\mathbf{A}^3\mathbf{G_t}^2\mathbf{R}^1$ is the scattering matrix belonging to this ray, which is scattered under the scattering angle θ. Because all Stokes vectors in one angular bin are simply added, neglecting their phases, also all the scattering matrices falling in the same angular bin may simply be added. After the raytracing is finished, the resulting scattering matrix $\mathbf{F}_{rt}(\theta)$ is normalized with respect to the total scattered energy and the solid angle element $d\Omega$ to yield the following normalization condition for the so-called phasefunction $p(\theta)$, which is the F_{11}-element of the scattering matrix:

$$\int p(\theta)d\Omega = 1 \tag{15}$$

Diffraction

Now, as the raytracing is done, the diffraction can be added. The diffraction does not change the state of polarisation of the incident radiation. This means that the same amount of energy is diffracted parallel and perpendicular to the scattering plane, and there is no phase difference between $I_{||}$ and $I_{\perp}$. These are the same conditions as for the Fresnel matrix but in addition, $\delta = 0$ and $a_1 = b_2 = d(\theta)$. The diffraction matrix is given by:

$$\begin{pmatrix} I_{\perp} \\ I_{||} \\ U \\ V \end{pmatrix} = d(\theta) \begin{pmatrix} 1 & 0 & 0 & 0 \\ 0 & 1 & 0 & 0 \\ 0 & 0 & 1 & 0 \\ 0 & 0 & 0 & 1 \end{pmatrix} \begin{pmatrix} I^o_{\perp} \\ I^o_{||} \\ U^o \\ V^o \end{pmatrix} = \mathbf{D} \begin{pmatrix} I^o_{\perp} \\ I^o_{||} \\ U^o \\ V^o \end{pmatrix} \tag{16}$$

The diffraction function $d(\theta)$ follows the same normalization condition as $p(\theta)$. Now the raytracing and diffraction matrices may be added in the following manner:

$$\mathbf{F} = \frac{1}{2\omega_o}\mathbf{D} + \left(1 - \frac{1}{2\omega_o}\right)\mathbf{F}_{rt} \tag{17}$$

ω_o is the single scattering albedo.

Change description of Stokes vector

As a last step, the notation of the Stokes vector has to be changed from $(I_{\perp}, I_{||}, U, V)$ to (I, Q, U, V). In one direction it is:

$$\begin{pmatrix} I \\ Q \\ U \\ V \end{pmatrix} = \begin{pmatrix} I_{||} + I_{\perp} \\ I_{||} - I_{\perp} \\ U \\ V \end{pmatrix} = \begin{pmatrix} 1 & 1 & 0 & 0 \\ -1 & 1 & 0 & 0 \\ 0 & 0 & 1 & 0 \\ 0 & 0 & 0 & 1 \end{pmatrix} \begin{pmatrix} I_{\perp} \\ I_{||} \\ U \\ V \end{pmatrix} = \mathbf{T} \begin{pmatrix} I_{\perp} \\ I_{||} \\ U \\ V \end{pmatrix} \tag{18}$$

and the other way round it is:

$$\begin{pmatrix} I_\perp \\ I_\parallel \\ U \\ V \end{pmatrix} = \begin{pmatrix} 0.5 & -0.5 & 0 & 0 \\ 0.5 & 0.5 & 0 & 0 \\ 0 & 0 & 1 & 0 \\ 0 & 0 & 0 & 1 \end{pmatrix} \begin{pmatrix} I \\ Q \\ U \\ V \end{pmatrix} = \mathbf{T^{-1}} \begin{pmatrix} I \\ Q \\ U \\ V \end{pmatrix} \tag{19}$$

Thus the transformation from the $(I_\perp, I_\parallel, U, V)$ representation which is used throughout the raytracing code, to the (I, Q, U, V) representation which is needed in the DAK model, has the following form:

$$\begin{pmatrix} I \\ Q \\ U \\ V \end{pmatrix} = \mathbf{T} \begin{pmatrix} I_\perp \\ I_\parallel \\ U \\ V \end{pmatrix} = \mathbf{TF} \begin{pmatrix} I_\perp^o \\ I_\parallel^o \\ U^o \\ V^o \end{pmatrix} = \mathbf{TFT^{-1}} \begin{pmatrix} I^o \\ Q^o \\ U^o \\ V^o \end{pmatrix} \tag{20}$$

and yields the new scattering matrix

$$\mathbf{F'} = \mathbf{TFT^{-1}} \tag{21}$$

3.2 Results for spheres

The results for spheres with and without absorption and with and without diffraction have been compared with results published in *Gish (1988)* and with Mie calculations. Figs. 3 and 4 show that there are no differences between the phasefunction and degree of linear polarisation as calculated in the former way (*COP-method*) and those calculated with help of the matrices described in Sect. 3.1 (*matrix-method*). F_{33}/F_{11} and F_{44}/F_{11} are shown in Fig. 5. They are equal as expected and agree very well with the results in *Gish (1988)* (not shown here) and with Mie calculations for a sphere with radius 1000 μm. The F_{22} element is always equal to F_{11} (not shown).

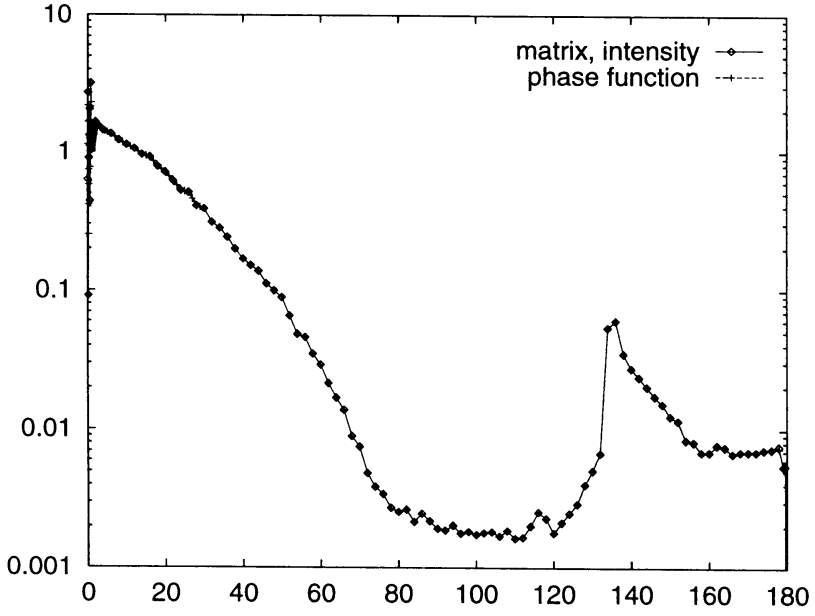

Figure 3: *Phasefunction F_{11} of a sphere (without diffraction) with refractive index 1.31-0i, calculated with and without use of matrices.*

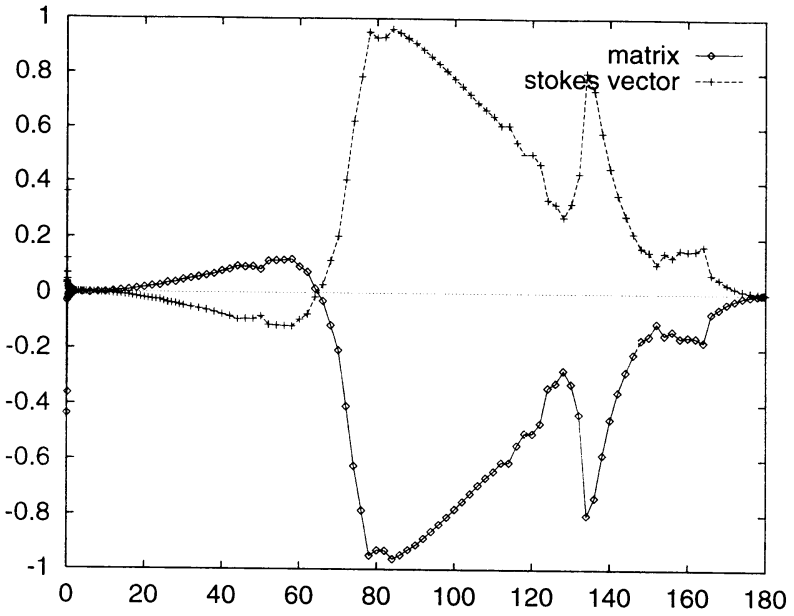

Figure 4: *Degree of linear polarisation* ($-F_{12}/F_{11}$) *for the phasefunction in Fig. 3. For the new matrix version* F_{12}/F_{11} *is shown.*

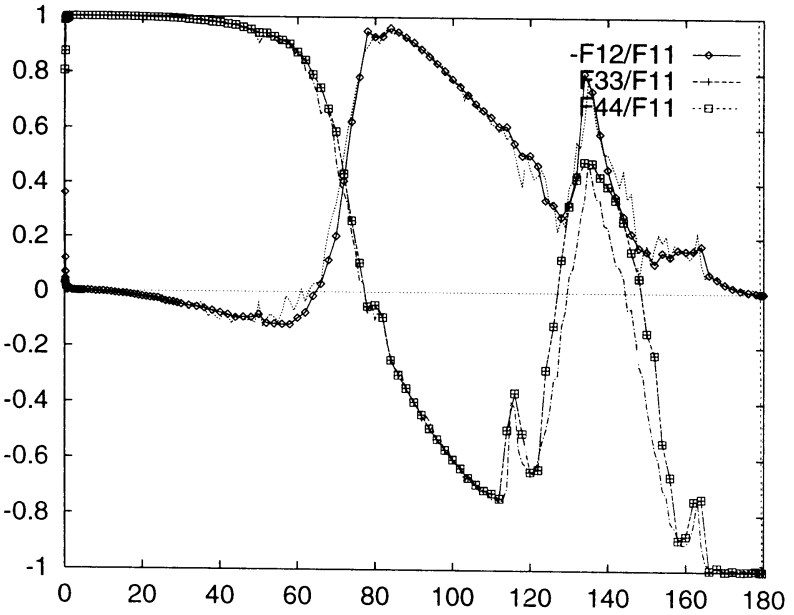

Figure 5: $-F_{12}/F_{11}$, F_{33}/F_{11}, *and* F_{44}/F_{11} *for the sphere in Fig. 3. The lines without symbols correspond to Mie calculations for a distribution of large spheres with a mode radius of 1000* μm.

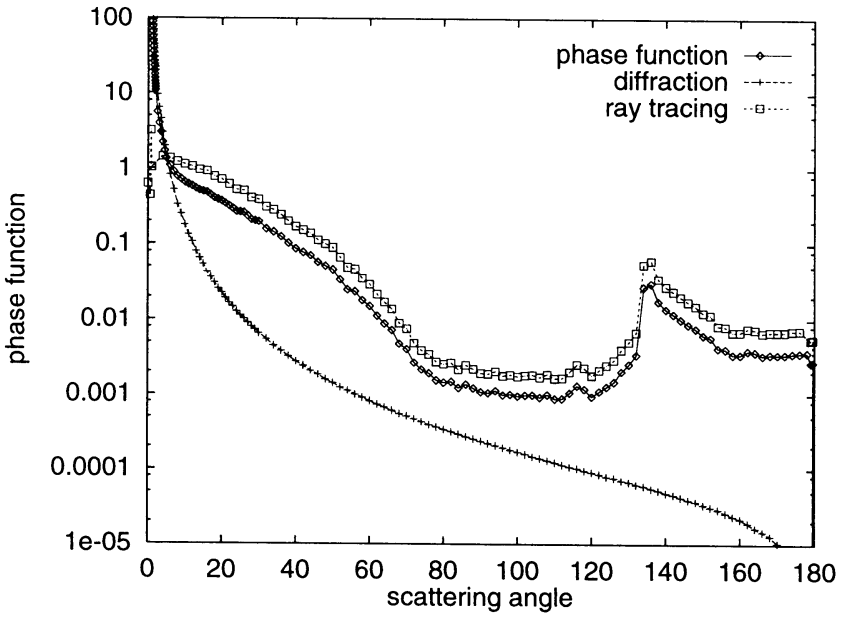

Figure 6: *Diffraction, raytracing and total phasefunction of a sphere with radius 10 μm and refractive index 1.31-0i at a wavelength of 0.5 μm.*

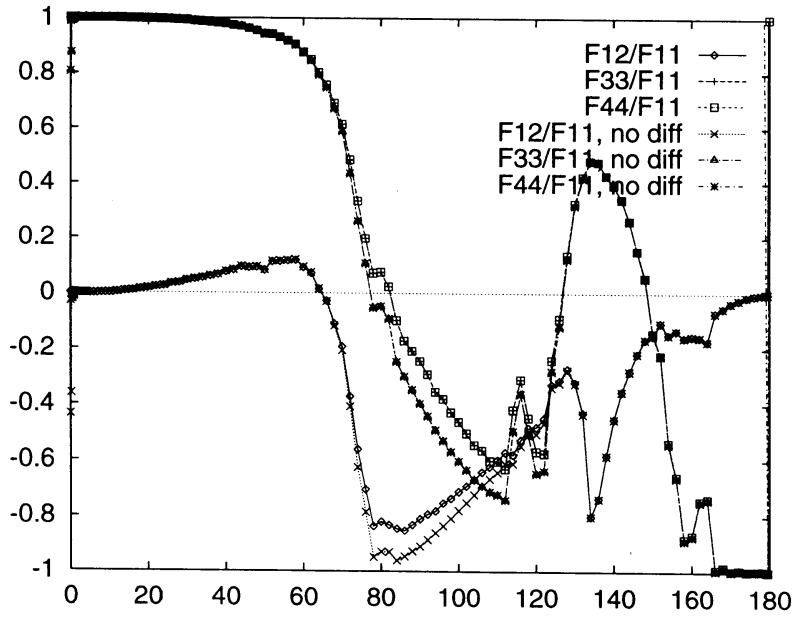

Figure 7: *Influence of diffraction on F_{12}/F_{11}, F_{33}/F_{11}, and F_{44}/F_{11} for the phasefunction in Fig. 6.*

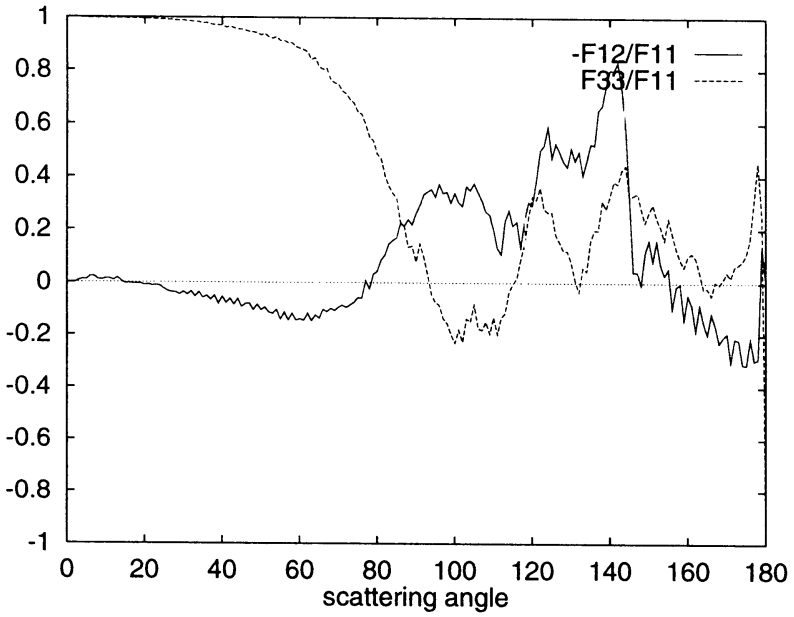

Figure 8: $-F_{12}/F_{11}$ *and* F_{33}/F_{11} *for the sphere used for Fig. 6, but calculated with Mie theory.*

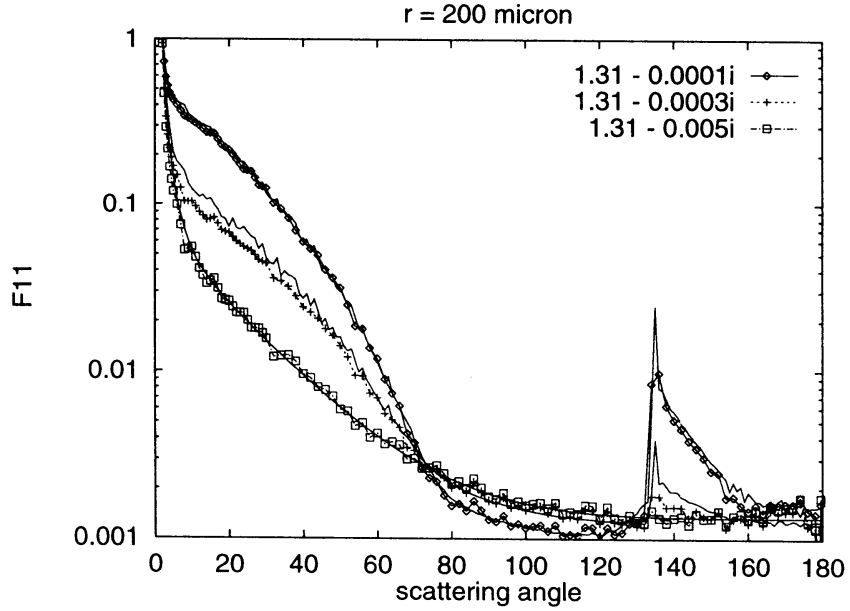

Figure 9: F_{11} *element of the scattering matrix for a sphere with a radius of 200* μm *at different values of absorption compared to Mie theory (curves without symbol).*

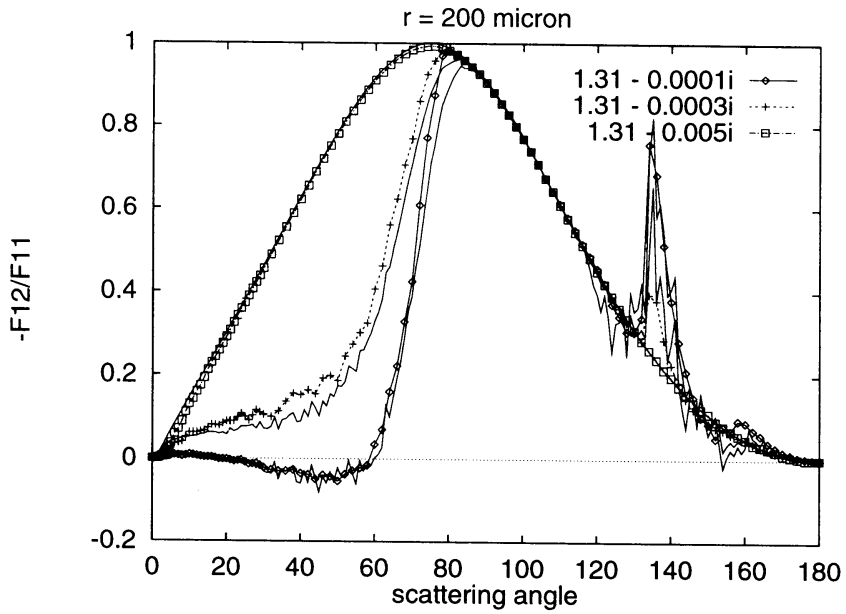

Figure 10: *Same as Fig. 9, but now for* F_{12}/F_{11}.

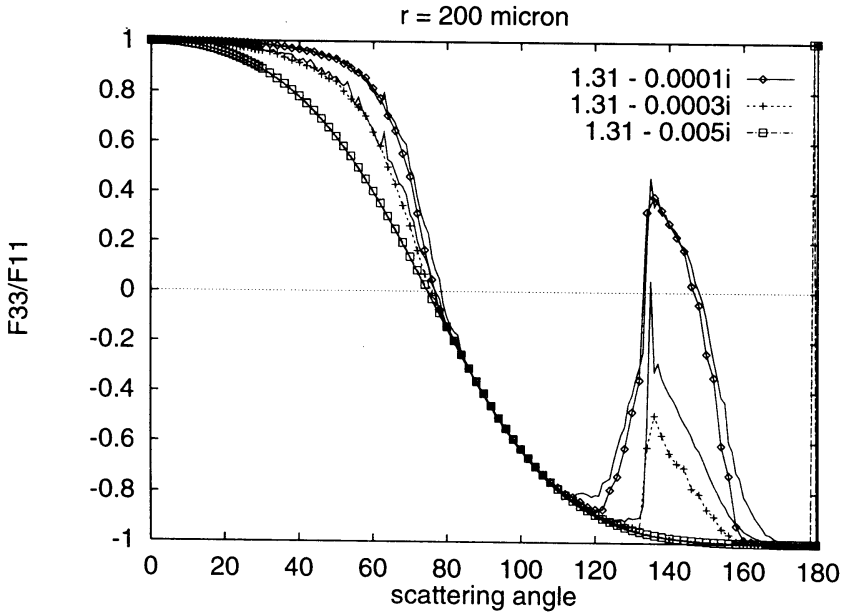

Figure 11: *Same as Fig. 9, but now for* F_{33}/F_{11}.

In Figs. 6 and 7 the influence of the diffraction is shown in an example for a nonabsorbing sphere with radius 10 μm. Fig. 6 shows the diffraction function for a 10 μm sphere, its raytracing function, and the sum of both, each function normalized to unity. It can be observed that the diffraction and raytracing functions are closest together in the forward scattering region up to 20° and in the side scattering region between 70° and 120°. Accordingly, the polarisation is mainly influenced between 70° and 120°. In forward scattering, there is not much polarisation, and therefore there is no influence of diffraction, too. This result is somewhat surprising, because usually one would not expect any influence of diffraction outside the forward scattering peak. It indicates that the geometric optics approximation is not valid for this relatively small sphere. For comparison, the F_{12}/F_{11} and F_{33}/F_{11} have been calculated with Mie theory also. The results are shown in Fig. 8; they are rather different indeed.

Calculations for a very large absorbing sphere are compared with Mie theory. Figs. 9, 10, and 11 show the independent non-zero elements F_{11}, F_{12}/F_{11}, and F_{33}/F_{11} of a scattering matrix for a sphere with radius 200 μm at low, medium, and strong absorption. The solid lines without symbols show Mie calculations for a size distribution with mode radius at 200 μm, and for a wavelength of 0.5 μm, corresponding to a size parameter of 2513, where the geometric optics approximation can safely be used. For all three elements there is a good agreement between raytracing and Mie theory for low and for strong absorption. At medium absorption there are small systematic deviations in the region between 10° and 60° and in the rainbow region. These differences are not due to insufficient statistics. The origin of these deviations could not be detected yet. Nevertheless, the overall behaviour of the dependence of scattering properties on absorption is well reproduced by the raytracing model. This result suggests that there are no principal errors in the algorithm for calculating the scattering matrix.

3.3 Results for randomly oriented hexagonal ice crystals

Since the results for spheres in Sect. 3.2 were satisfactory, the program version for calculating scattering matrices for spheres has been combined with the former version for calculating phasefunctions of hexagonal particles, to form a new code for calculations of scattering matrices of spheres and hexagonal particles. The scattering matrices of hexagonal particles have been compared qualitatively with data published by *Takano and Jayaweera (1985)* and quantitatively with results made available by *Macke (priv. comm.)*. The results of the latter comparison are shown in the following figures. First, the raytracing part of the phasefunction (without diffraction) is compared in Fig. 12. The differences in the halo regions are due to the different angular resolutions used in both codes. Another deviation occurs around 170° scattering angle. Here, a small peak is missing in the phasefunction of Macke, which always had been there in former comparisons. This could be due to a restriction in the maximum number of interactions of a ray with the crystal faces applied in the calculation of Macke. This deviation leads to corresponding differences in some of the other matrix elements. These elements are shown in the remaining parts of Fig. 12. They are not discussed in detail, because the general correspondence is very good, but just a few features will be mentioned. The F_{12}/F_{11} functions show deviations around the 22° halo, which reflect differences in the diffraction function (see later) and/or in the way in which the rays in the δ forward transmission peak are treated. Furthermore, F_{34} element of Macke has the wrong sign *(Macke, priv. comm. 1997)*. The diffraction calculations have also been compared with the code of Macke at this opportunity. They are now nearly identical after the removal of some differences, which showed up in the beginning of the comparison (cf. Fig. 12).

Fig. 13 shows the contribution of different ray paths to the scattering matrix of a columnar crystal at a wavelength of 550 nm and for a maximum tilt angle (cf. Sect. 4) of 1°. Each curve corresponds to a certain maximum number of possible interactions of ray and crystal surface. If only externally reflected rays are considered, the result is the same as external reflection at a sphere. Adding twice refracted and thus transmitted rays to the external reflection yields the haloes in the scattering function and related features in F_{33}/F_{11} and F_{12}/F_{11}. The F_{44} element, which equals zero for external reflection, now

becomes the same as the F_{33} element, while F_{22}/F_{11} remains nearly unchanged and equal to 1. The F_{43} element is unchanged and equal to zero. Further adding one internal reflection yields additional scattering at all scattering angles larger than about 40°. This is accompanied by a reduction of the linear polarisation from 1 at the Brewster angle to less than 0.5 at all scattering angles. The F_{33} and F_{44} elements are still equal to each other. With two internal reflections added, the maximum of the scattering function at 150° appears together with related features in all other matrix elements except in the linear polarisation. With three internal reflections, the final general shape is reached for all matrix elements. Further internal reflections still introduce changes in the matrix elements and may even add small features in the scattering function, such as the maximum at 170° which can not be seen in this figure. However, the general shape of the scattering matrix is not affected by adding more internal reflections.

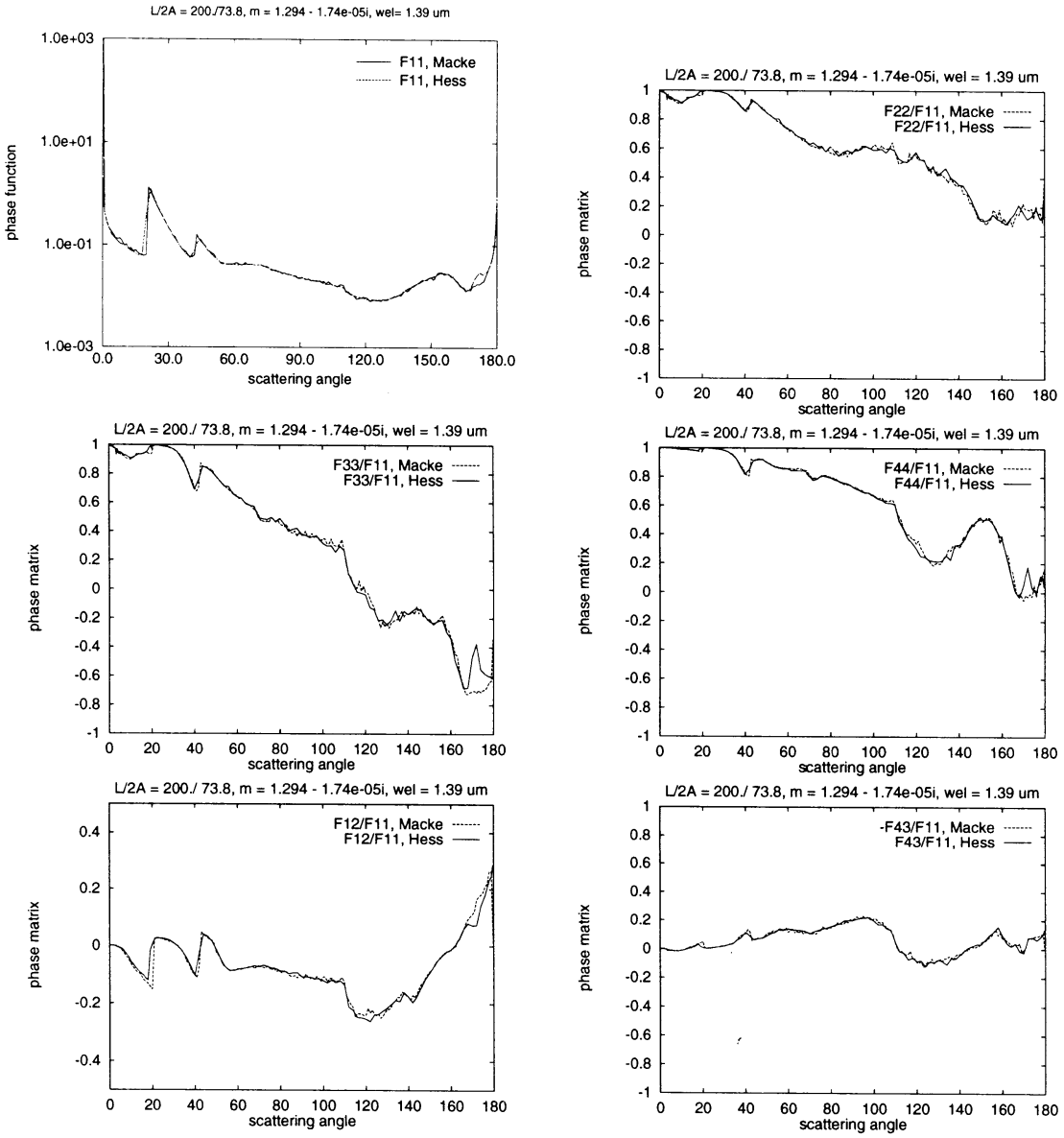

Figure 12: *Scattering matrix elements of a hexagonal ice column in comparison with results of Macke. In this figure, diffraction is included except for the* F_{11} *element.*

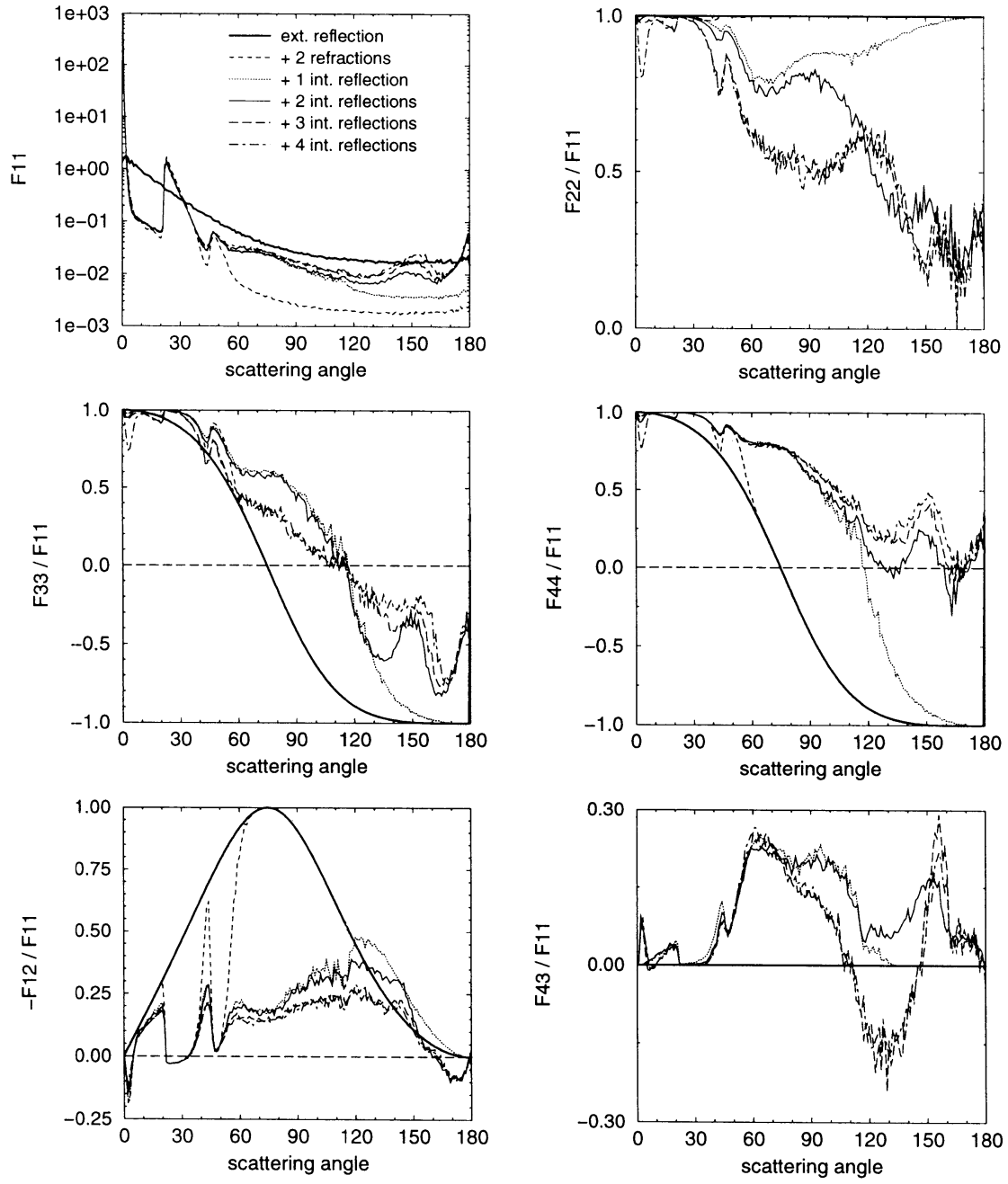

Figure 13: Contributions of various ray paths to the scattering matrix elements of a hexagonal ice crystal. The ice crystal has an aspect ratio of 5.9. The maximum tilt angle is 1° (cf. Sect. 4). The wavelength is 0.55 μm.

4 Statistical variation of ray paths

Real crystals in cirrus clouds very seldom show the exact hexagonal shape, which is used in the raytracing calculations. This comes in addition to the fact that the crystals may have many different shapes depending on the growing conditions (see classification by *Magono and Lee (1966)*). They may show deviations from the idealized shapes and may have angles between the crystal surfaces which differ from 60° or 90°, and their surfaces often are no perfect planes. Because of this large variability, it is not possible to apply a detailed realistic ice crystal model to cirrus clouds. It is necessary to select one or a few particle shapes as representative shapes for ice cloud particles, which are at least representative with respect to the optical properties. Out of all possible shapes, the hexagonal columns and plates have been chosen in the present work to be representative for most conditions in cirrus clouds, regardless of what special crystal shapes really occur. The reasons for this choice are that these are the basic shapes of ice crystals growing under undisturbed conditions, and that they produce most of the known halo phenomena in cirrus clouds.

However, it is well known that these idealized crystals yield single scattering properties, which are not always suited to describe the radiative properties of cirrus clouds. For this reason, *Macke et al. (1996)* developed the *polycrystals*, which improved in many cases the modelling of radiative properties compared to measurements. In the present work, a different approach is used, which also has been proposed by *Macke et al. (1996)*, but was not followed further. This method is described in the following.

To allow for the above mentioned arbitrary deviations from the idealized particle shape, a limited statistical variation of the ray directions during the raytracing procedure is applied and meant to make the model more realistic, because it will wash out those features of the phasefunction which are closely related to the idealized particle shape.

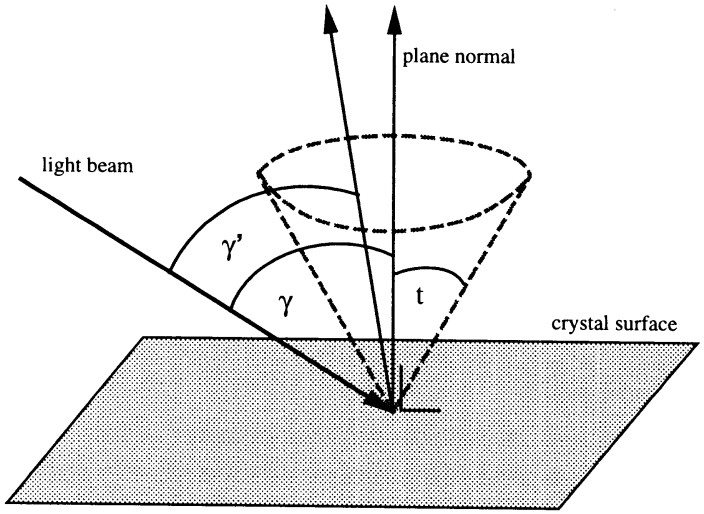

Figure 14: *Geometry of the tilting of plane normals. The angle t is the maximum tilt angle, γ is the angle of incidence, and γ' is the new angle of incidence after tilting the plane normal.*

Each time a ray hits a crystal face, the normal to this plane is shifted randomly around its original direction (Fig. 14). The angles between the former and the new directions are distributed uniformly between zero and a given maximum tilt angle t and the azimuth around the original direction is chosen to be uniformly distributed between 0 and 2π. Thus, the probability density for ray paths near the original path is larger than that for large deviations because the solid angle intervals around zero

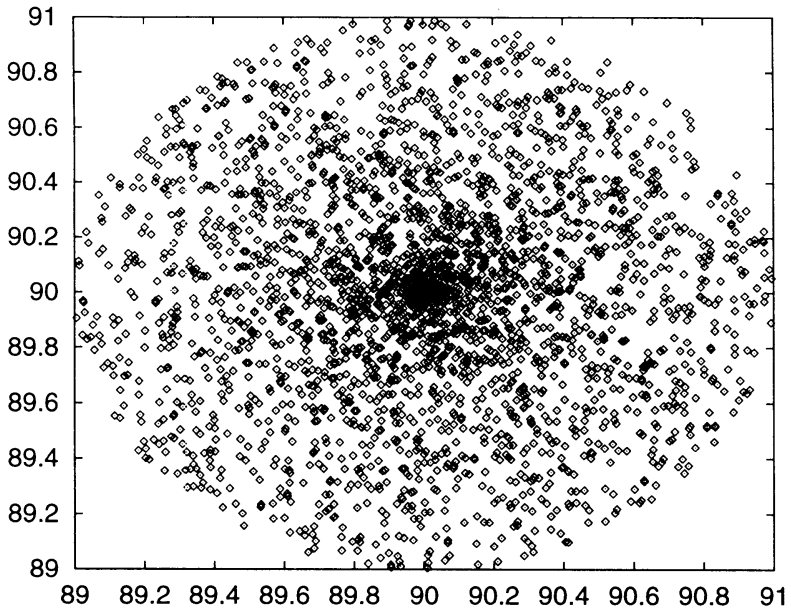

Figure 15: *Coordinates of 4000 realisations of a unit vector, which is shifted randomly by up to 1° from its original direction perpendicular to the page.*

deviation are smaller than at larger angles (see Fig. 15). This method corresponds more to a certain roughness of the crystal surface than to a distortion of the crystal geometry. The small surface element of the crystal surface where it is hit by the ray changes its orientation, while the overall geometry of the particle is not affected. Please note that there is no multiple external reflection between the tilted surface elements taken into account and of course there is no attention paid to wave phenomena which should occur at such very small features at the surface.

This approach is different from another possibility, which would consist of random changes of the crystal geometry. In this case, each ray hits a somewhat different crystal with a well-defined shape. This shape is distorted in comparison with the ideal crystal shape. This second method has not been chosen for the present work, because the raytracing code makes explicitly use of the ideal hexagonal geometry.

4.1 Changes in raytracing code

The raytracing code had to be modified in two places to realize the tilting of the plane normals. Firstly, the random change of the direction of the plane normals itself had to be introduced, and secondly, the calculation of the new direction of rays after an interaction with a crystal face had to be adapted.

- **random change of plane normal**

  For the purpose of tilting the plane normal a new subroutine was introduced, which is called whenever a ray hits the particle surface and if the given maximum tilt angle is larger than zero. In this subroutine the formulae are contained which are needed to rotate the direction of a vector over a given polar rotation angle θ and a given rotation azimuth angle ϕ:

$$\begin{aligned} xx &= \sin(\theta)\ \cos(\phi)\ zx^{\circ} + \sin(\theta)\ \sin(\phi)\ yx^{\circ} + \cos(\theta)\ xx^{\circ} \\ xy &= \sin(\theta)\ \cos(\phi)\ zy^{\circ} + \sin(\theta)\ \sin(\phi)\ yy^{\circ} + \cos(\theta)\ xy^{\circ} \\ xz &= \sin(\theta)\ \cos(\phi)\ zz^{\circ} + \sin(\theta)\ \sin(\phi)\ yz^{\circ} + \cos(\theta)\ xz^{\circ} \end{aligned} \tag{22}$$

(xx^o, xy^o, xz^o), (yx^o, yy^o, yz^o), and (zx^o, zy^o, zz^o) are the axes of a coordinate system where (xx^o, xy^o, xz^o) is the usual, undisturbed direction of the plane normal of the crystal surface. This coordinate system is given relative to the fixed coordinate system used throughout the raytracing procedure. (xx, xy, xz) is the plane normal after tilting. The angles θ are randomly distributed between zero and the given maximum tilt angle and ϕ is chosen to be equally distributed between zero and 2π. After calculating the new direction of the plane normal, the angle of incidence on the new, tilted crystal face is calculated and the directions of the refracted and reflected rays are determined as before.

- **new ray direction after interaction with crystal face**

  For the calculation of the new ray direction after the interaction with the crystal face, there was a restricted formulation in use, which made use of the hexagonal particle geometry. Since this fixed geometry is disturbed by the tilting, in this case a more general formulation has to be used. To calculate the three coordinates of the new ray direction, three independent equations are needed. The following are used, according to Fig. 2:

$$\vec{b_t} \cdot \vec{f} = \cos(\theta_t) \text{ or } \vec{b_r} \cdot \vec{f} = \cos(\pi - \theta_i) \tag{23}$$

  the angles θ_t and θ_i between the refracted ray $\vec{b_t}$ or the reflected ray $\vec{b_r}$ respectively, and the plane normal $\vec{f}$ are known from Snell's law.

$$\vec{b_t} \cdot \vec{a} = \cos(\theta_{d_t}) = \cos(\theta_i - \theta_t) \text{ or } \vec{b_r} \cdot \vec{a} = \cos(\theta_{d_r}) = \cos(\pi - 2\theta_i) \tag{24}$$

  the angles between the incoming ray $\vec{a}$ and the refracted and reflected rays are also known.

$$(\vec{b} \times \vec{a}) \cdot \vec{f} = 0 \tag{25}$$

  this condition means that the vectors $\vec{a}$, $\vec{b}$, and $\vec{f}$ are all in the same plane. The angles θ_i (angle of incidence) and θ_t (refraction angle) are known, as well as the directional vectors $\vec{a}$ (incoming direction) and $\vec{f}$ (plane normal). $\vec{b}$ is the direction of the refracted or reflected ray which we want to know. These three equations form a system of linear equations for $\vec{b}$, which is solved with help of a LAPACK-subroutine

$$\begin{pmatrix} f_1 & f_2 & f_3 \\ a_1 & a_2 & a_3 \\ (a_2 f_3 - a_3 f_2) & (a_3 f_1 - a_1 f_3) & (a_1 f_2 - a_2 f_1) \end{pmatrix} \begin{pmatrix} b_{t1} \\ b_{t2} \\ b_{t3} \end{pmatrix} = \begin{pmatrix} \cos(\theta_t) \\ \cos(\theta_i - \theta_t) \\ 0 \end{pmatrix} \tag{26}$$

  The values a_1, f_1, b_{t1} are coordinates of the vectors $\vec{a}$, $\vec{f}$, $\vec{b_t}$. A corresponding equation holds for the reflected ray.

- **check for consistency**

  By applying this method it may happen that for instance an internally reflected ray leaves the crystal, because the tilt angle of the actual surface element was too large. In the same way, it may happen that a ray which is supposed to be refracted out of the crystal, actually cannot leave the crystal. The reason for this behaviour is that the geometry of the crystal is not changed by this method. The borders of the particle are assumed to remain the same. To avoid such wrong ray paths, the angle between the new ray direction and the original, untilted plane normal of the surface element is checked. If it is larger than 90° for the refracted ray or less than 90° for the reflected ray, the tilt angle is refused and a new one is applied. The largest tilt angle which still yields possible ray paths is only dependent on the incident angle and the refractive index. The method used here yields a uniform distribution of tilt angles between zero and the maximum tilt angle t or the largest possible tilt angle, if the latter is smaller than t.

4.2 Results

Fig. 16 shows the raytracing part of the scattering matrix of a large columnar crystal (110 μm/1300 μm) at a wavelength of 550 nm and for different maximum tilt angles (cf. Sect. 4). The smallest tilt angle of 1° only affects the forward and backscattering directions. With increasing tilt angle, the halos in the phasefunction become less pronounced and the 22° halo vanishes at a maximum tilt angle of 30°. At this tilt angle, also the maximum at 150° vanishes, while the backscattering maximum between 170° and 180° already lacks at a tilt angle of 10°. Increasing the maximum tilt angle further than 60° does not introduce large further changes to the phasefunction.

This behaviour is in principle the same for particles with different aspect ratio. It is also similar for the other elements of the scattering matrix. At 30° tilt angle, the slope of the curves is completely changed compared to the curves for 0° tilt angle. A further increase of the maximum tilt angle shows this new slope more distinctly, but does not change the general behaviour any more.

The calculations shown here may be compared to results of *Macke et al. (1996)*. Their Fig. 8 shows results which seem to be calculated, according to their description, with the same assumptions as the scattering matrix in Fig. 16 of the present report. The overall behaviour indeed is the same for the phasefunctions. However, there seems to be a difference in the definition of the distortion parameter or tilt angle, because Macke et al. get similar effects with about half the tilt angle. In their polarisation figure, there is no effect on polarisation in the side scattering region, while the calculations presented in this report show a noticeable effect for the 10° tilt angle. Also Macke et al. still get negative polarized backscattering, while the calculations presented in this report show neutral polarized backscattering for all tilt angles larger than 1°. At the moment the cause of the difference between the two methods is not clear.

For comparison, the same type of calculations is shown for spheres in Fig. 17. In this case, the general slope of the curves is not changed because of the tilting of the plane normals, but all the rainbow features are washed out in the phasefunction. In the polarisation they remain visible, but are shifted to somewhat smaller scattering angles in case of the F_{33} element. The maximum in the degree of linear polarisation at the rainbow angles is first shifted to larger scattering angles and then, for maximum tilt angles larger than 30°, it is shifted to smaller scattering angles. It is interesting to note that the number of independent non-zero matrix elements remains three.

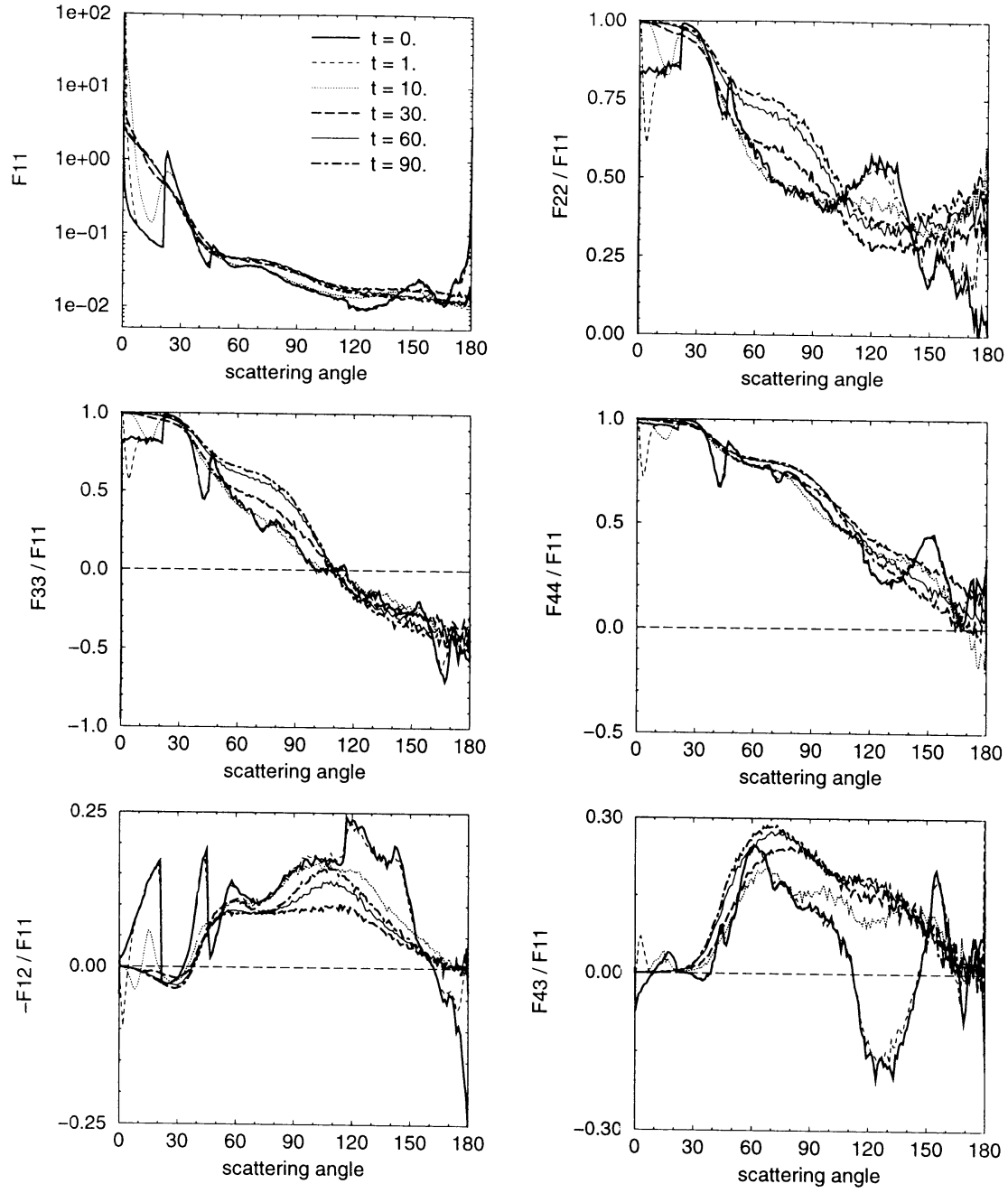

Figure 16: *Scattering matrix elements of ice crystals with different maximum tilt angles (in degrees). The ice crystals are hexagonal columns with an aspect ratio of 5.9. The wavelength is 0.55 μm. No diffraction is included here.*

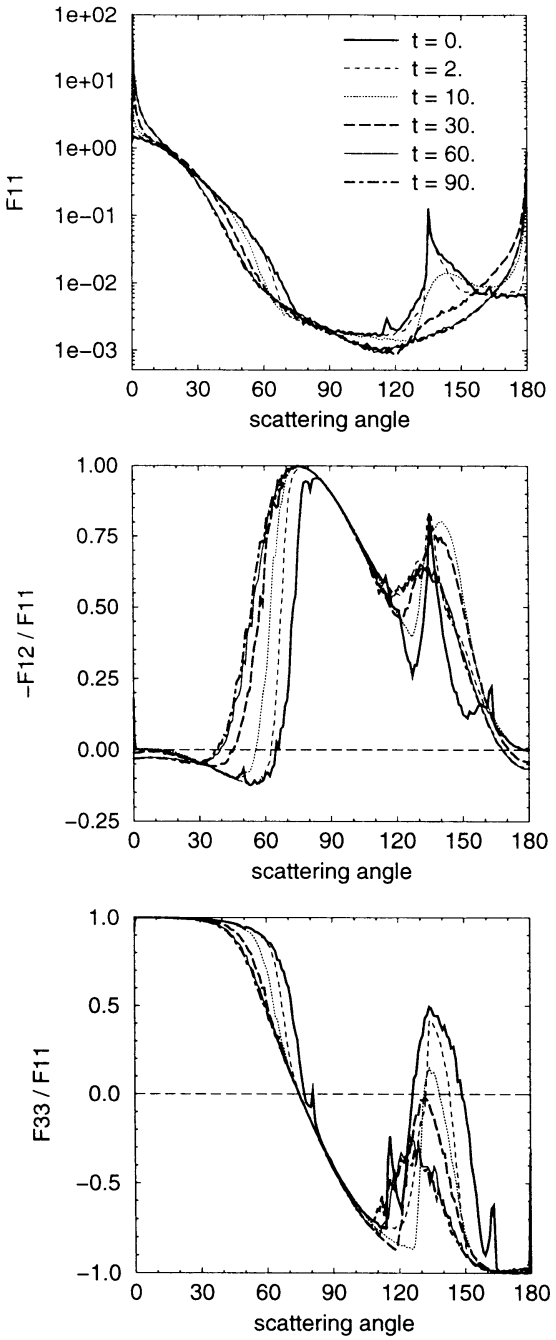

Figure 17: *The non-zero elements of the scattering matrix for a sphere at different tilt angles. No diffraction is included here. The wavelength is 550 nm (no absorption).*

5 Additional improvements of the raytracing code

In addition to the main enhancements of the raytracing code, which have been addressed in the former chapters, many minor improvements have been introduced. The two most important ones are described in the following.

5.1 Test of convergence

The convergence of the raytracing procedure is followed continuously during the execution of the program. For this purpose, the phasefunction is calculated each time after a certain number of rays has been traced. The phasefunction then is compared to the previous realisation. The program stops if the difference at all angles is less than a specified value; otherwise it is continued until a given maximum number of rays is reached. For this purpose, three new values are introduced in the input file:

- the question: "use convergence test?" has to be answered with yes or no. "no" means that the raytracing is continued until the given maximum number of rays is reached.
- the convergence criterion must be given. This is a number between 0 and 1 and gives the maximum tolerated relative deviation between two successive realizations of the phasefunction. The first time this value is reached at the same time for all angular bins, the raytracing is stopped. If the maximum number of rays is reached without convergence having taken place the program is terminated as well.
- the number of rays must be given after which a new phasefunction is calculated. This number must be large enough to produce a roughly reliable phasefunction itself. So at least 50,000 or 100,000 rays are required here. Using a convergence criterion of 0.01 will lead to at least 3,000,000 rays. Fig. 18 shows the dependence of the number of rays needed on the chosen convergence criterion and on the incremental number of rays between two convergence tests. It can be observed that a small increment in ray number (1000) yields a rather fast convergence. An increment of 100,000 rays between two successive calculations of the phasefunction should be used for the convergence criterion. In this case a total number of rays of 1,000,000 will be enough to get a maximum error of about 5%.

5.2 New random number generator.

A new random number generator is applied, because there is evidence that the formerly used random numbers are not good enough, especially when more than 1,000,000 rays are used. According to *Numerical Recipes*, simple kinds of random number generators do show sequential correlation on successive calls. For this reason, the FUNCTION RAN3 of *Numerical Recipes* is now used in the raytracing code.

With use of this new function, the apparently wrong scattering functions that were the result of a calculation with more than 1,000,000 rays did not occur. Nevertheless, only the uniform distribution between 0 and 1 has been checked for the new random numbers (see Fig. 19).

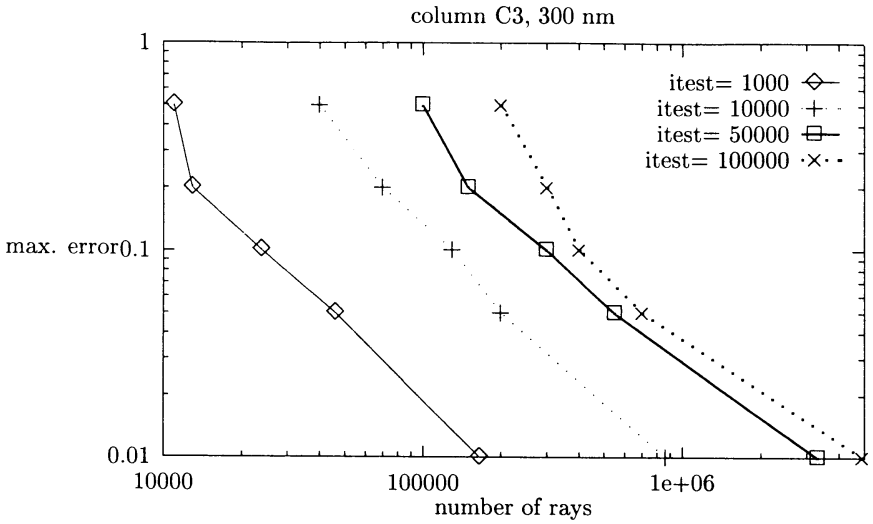

Figure 18: *Number of rays needed to achieve an accuracy better than the given maximum error.*

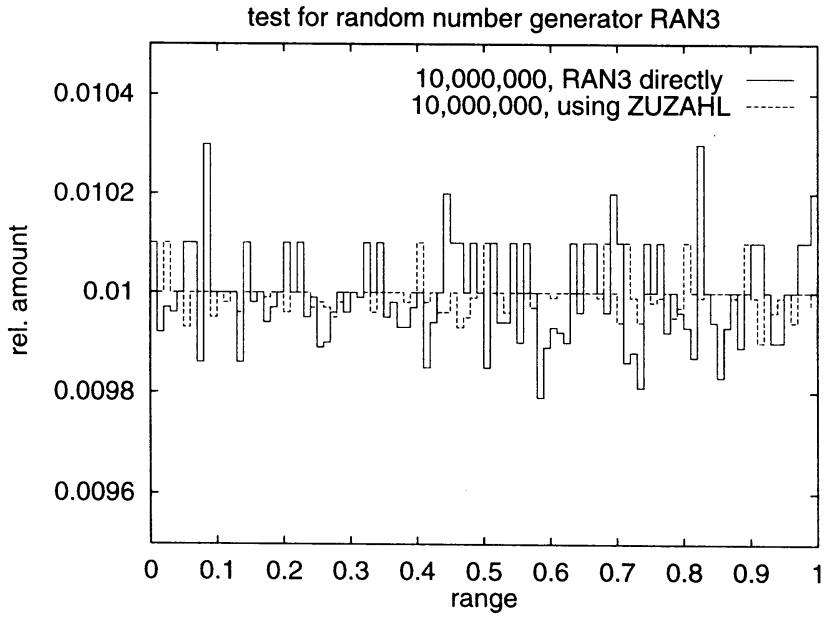

Figure 19: *Distribution of random numbers between 0 and 1. This range has been divided in 100 intervals. Therefore the relative amount in each interval should be 0.01. ZUZAHL is the subroutine, which calls the random number generator FUNCTION RAN3.*

6 The database

For further use, scattering matrices of a number of particle sizes and shapes at various wavelengths must be calculated and stored. In addition, the use of size distributions must be possible. As a first step, this database will have a structure similar to the COP database *(Hess and Wiegner, 1994)*. Calculations for 8 single particles in the size range from 2 μm to 2000 μm are stored for several wavelengths. With help of an additional code these optical properties of single particles may be mixed to yield optical properties of a cirrus cloud by use of cirrus size distributions.

6.1 Particle sizes

The particle sizes which are used in the program are shown in Table 1 *(Hess, 1996)*. They are the same as those used in the COP database. The increase of the particle's aspect ratio with size is modelled after formulae which were fitted to a large number of measurements by *Auer and Veal (1970)*.

It should be noted that the presupposed laws of geometric optics are not strictly valid for the small ice crystals. However, since in the particle size limit at which the geometric optics approximation breaks down is unknown in case of ice crystals, calculations are performed for the smaller crystals as well. Moreover, there is still no other practicable way to get scattering matrices for ice crystals, which are not large enough for geometric optics, but too large for Rayleigh scattering.

Table 1: *Sizes of the ice crystals used by* coma

intervall No.		b	a	1	2	3	4	5	6
interval boundaries [μm]		2..6	6..20	20..40	40..90	90..200	200..400	400..900	900..2000
columns	A [μm]	1.4	4.	10.	22.	41.	60.	80.	110.
	C [μm]	3.5	10.	30.	60.	130.	300.	600.	1300.
	C/2A	1.25	1.25	1.5	1.4	1.6	2.5	3.8	5.9
plates	A [μm]	-	-	15.	30.	65.	150.	300.	650.
	C [μm]	-	-	9.	12.	17.	24.	33.	47.
	C/2A	-	-	0.3	0.2	0.13	0.08	0.055	0.036

6.2 Particle shapes

As standard particle shapes the ideal hexagonal columns and plates are used. These particles have several disadvantages due to their ideal shape, which restrict their usefulness for cloud research. Therefore, crystals with a certain surface roughness, as discussed in section 4, are used as well. There are three features in the phasefunctions of ideal hexagonal crystals which limit their use for practical applications:

- **the δ peak in the direct forward direction ($\theta = 0$).**

  This peak does not contribute to numerical integrals of the phasefunction and therefore yields wrong normalization and wrong asymmetry parameters. For the ideal crystals this error is avoided by considering the energy going in this direction as being not scattered at all. Consequently, the scattering coefficient and all other related quantities are changed compared to the pure raytracing results.

- **the δ peak in the direct backward direction ($\theta = 180$).**

  This peak is caused by reflection at 90° angles between crystal planes. The phasefunction value at 180° depends mainly on the size of the last angular bin of the raytracing phasefunction. This value is important for interpretation of lidar measurements.

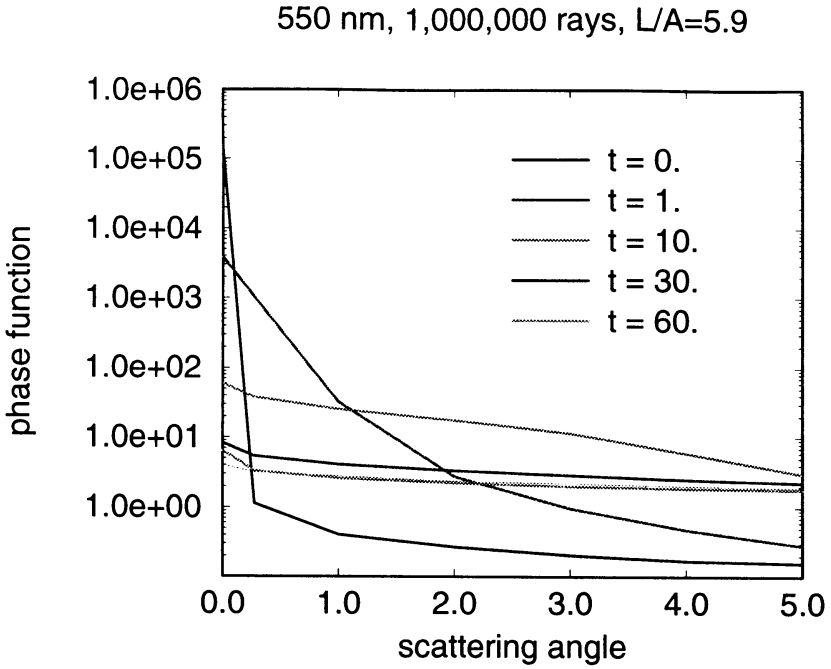

Figure 20: *Forward scattering for a column with size 110 μm / 1300 μm at a wavelength of 0.55 μm for different maximum tilt angles.*

- **the halos at 22° and 46°.**

  The ideal crystals always show pronounced halos, while there are very seldom halos observed in natural cirrus clouds.

The degree of statistical variation which is needed to avoid these problems, and which therefore will be applied in further studies, can be determined by inspection of Figs. 16, 20, and 21, and can be summarised as follows:

- To avoid the forward and backward δ peaks, a tilt angle of 1° is sufficient (cf. Figs. 20 and 21). Therefore, this is a model for nearly ideal hexagonal columns, only avoiding some numerical inconveniencies.
- A tilt angle of 30° washes out all halo features of the original phasefunction. Therefore, this may serve as a model for non-ideal random hexagonal particles.

The influence of the particle's aspect ratio on the scattering matrix elements is shown in Fig. 22. Here, the scattering matrix of a column with very small aspect ratio (1.25, corresponding to a very small particle) is compared to that of a column with large aspect ratio (5.9, for a very large particle). In both cases a maximum tilt angle of 30° is applied. There is no diffraction included in this figure. It can be seen very clearly that the influence of the aspect ratio remains present, although the rather large maximum tilt angle has washed out all the special features belonging to the hexagonal geometry. The effect that large tilt angles wash out the special shape related features of the matrix elements has also been shown for spheres (Fig. 17). In Fig. 23 the polycrystals of Macke and a platelike crystal are shown in addition to the two columns from Fig. 22. For all matrix elements, the polycrystals shows a behaviour similar to the two roughened columns, while the roughened plate yields rather different matrix elements.

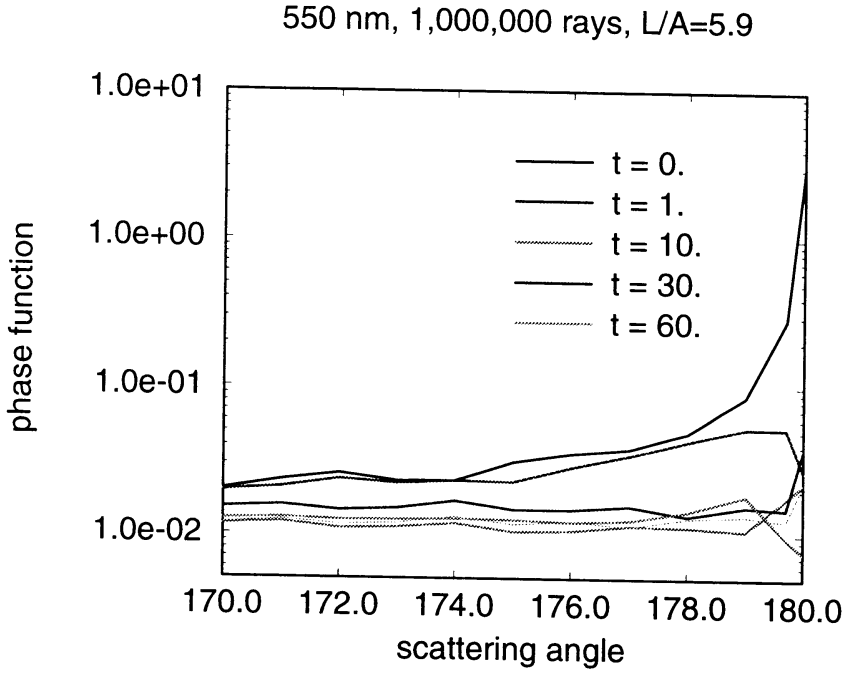

Figure 21: *Back scattering for a column with size 110 μm / 1300 μm at a wavelength of 0.55 μm at different tilt angles.*

Fig. 24 shows the asymmetry parameters of the hexagonal crystals in Fig. 23 in dependence of the maximum tilt angle. The asymmetry parameter of the polycrystals is 0.74 and nearly independent of particle size. The asymmetry parameter curves of the columnar crystals show a minimum near 30° maximum tilt angle; the smaller crystal nearly reaches the low value of polycrystals. In case of the platelike crystal no minimum occurs, and the asymmetry parameter remains constant for maximum tilt angles larger than 30°. Thus this figure also suggests that a maximum tilt angle of 30° is a useful value to represent scattering at non-ideal hexagonal crystals.

This last figure especially is an indication for the usefulness of the "roughened" columns, because they offer two free shape parameters more than the polycrystals, namely the aspect ratio of the column and the degree of "roughness". This could help in the interpretation of radiation measurements which could not be explained sufficiently with neither polycrystals nor hexagonal particles. Presently, the database contains calculations for columnar ice crystals with maximum tilt angles of 1° and 30°.

6.3 Size distributions

For weighting the scattering properties of single particles with cirrus particle size distributions, the program COMA can be used. As size distributions, the eight distributions given by *Heymsfield and Platt (1984)*, which are based on measurements, may be used as well as the parametrization with cloud temperature given by *Liou (1992)*, which is based on the same measurements. These distributions are only valid for particles with a maximum dimension larger than 20 μm, since there were no reliable measurements below this size. These distributions have the form:

$$\begin{aligned} \frac{dN}{dx} &= a_1 x^{b_1} I \; for \; x < x_o \\ \frac{dN}{dx} &= a_2 x^{b_2} I \; for \; x > x_o \end{aligned} \tag{27}$$

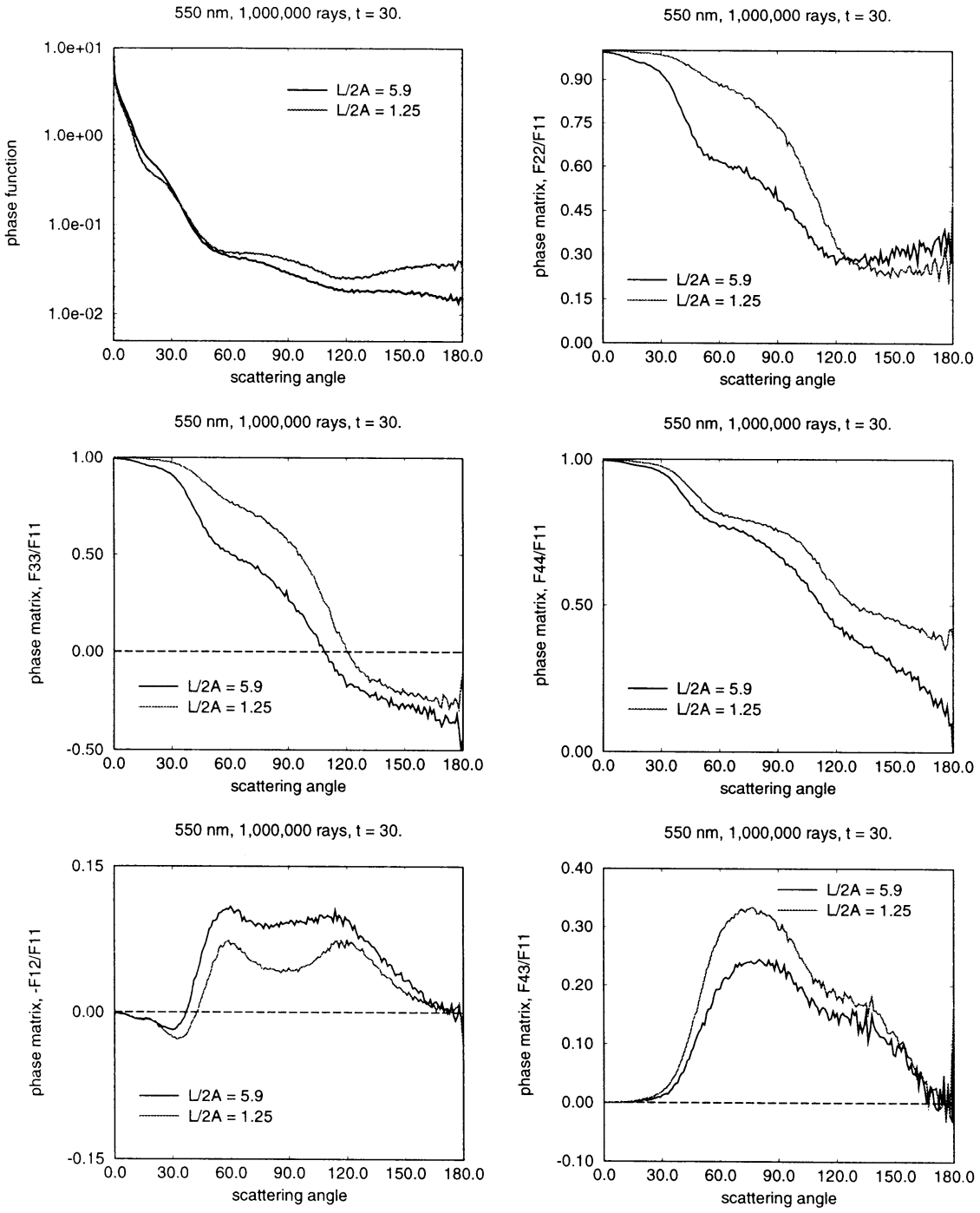

Figure 22: *Raytracing part of the scattering matrix for two columns with different aspect ratios at a wavelength of 0.55 μm and at a maximum tilt angle of 30°.*

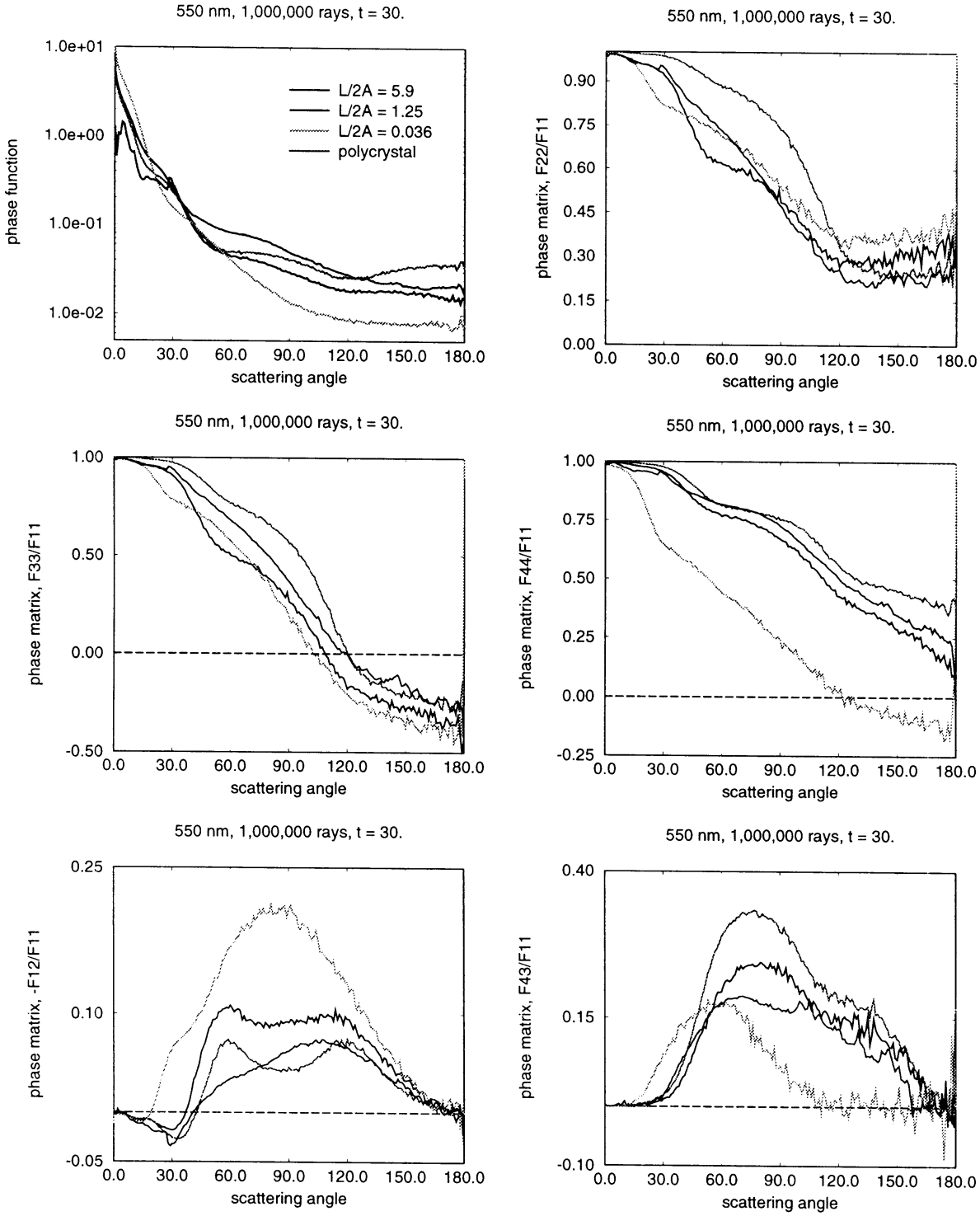

Figure 23: *Same as Fig. 22, but with polycrystals and platelike crystal additionally.*

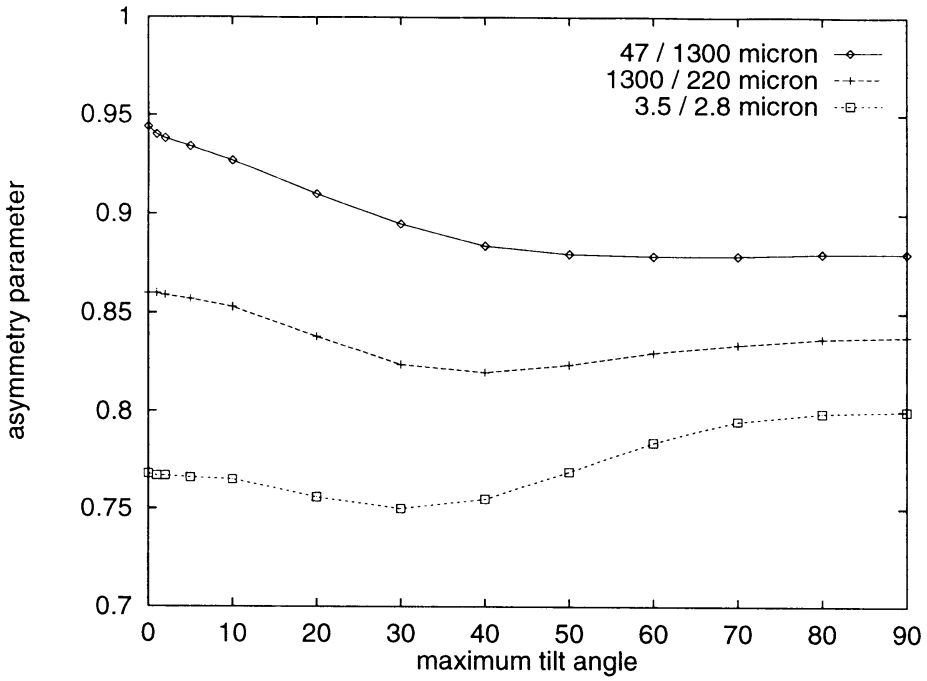

Figure 24: *Asymmetry parameter of hexagonal crystals as function of the maximum tilt angle. Different curves pertain to different particles. The wavelength is 0.55 μm. The polycrystals have an asymmetry parameter of 0.74.*

where the coefficients $a_{1,2}$ and $b_{1,2}$ and the ice water content I are functions of cloud temperature. The program COMA also allows the use of discrete values of particle number density for the 8 size intervals in the database.

6.4 Wavelengths

At the moment, the database contains calculations for columnar ice crystals at the following ATSR-2 wavelengths: 0.55 μm, 0.66 μm, 0.87 μm, 1.6 μm, and 3.7 μm.

Fig. 25 shows the influence of the absorption on the scattering matrix. Absorption does not influence the externally reflected part, while there will be less energy scattered by those rays which have been transmitted through the crystal. Therefore, the weight of the external reflection becomes stronger when absorption takes place.

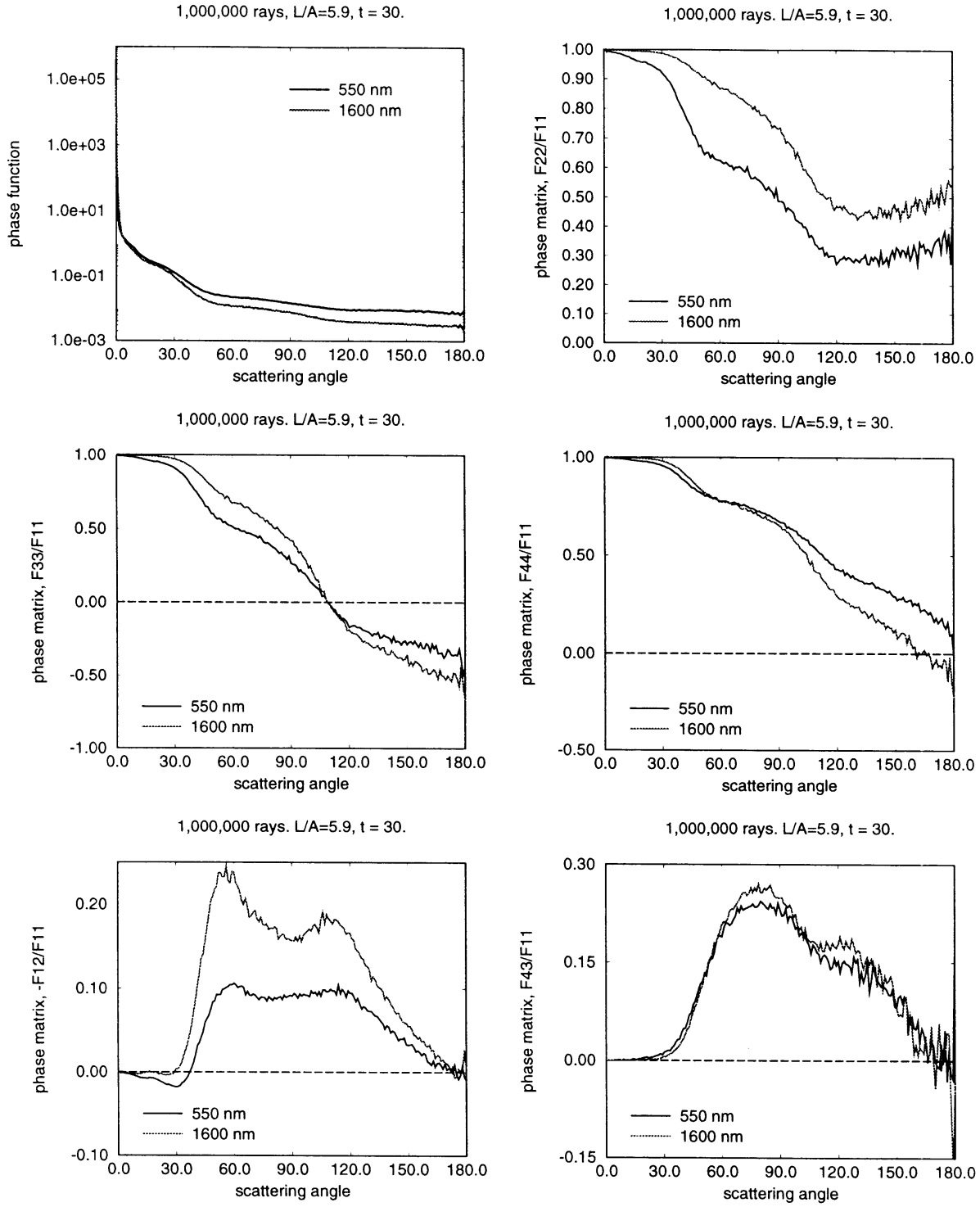

Figure 25: *Comparison of the scattering matrix elements of a hexagonal ice column at two wavelengths, one without absorption (0.55 μm) and on with absorption (1.6 μm). In this figure diffraction is included.*

7 Expansion coefficients

For use in the radiative transfer model DAK, the scattering matrix has to be expanded in generalized spherical functions (see e.g. *de Rooij and van der Stap, 1984*). This is done by use of an existing code, which is adapted to the raytracing code and included as a subroutine. This subroutine produces the output needed as input for the DAK model. Thus, an interface exists between the raytracing code and the DAK model.

7.1 Delta approximation

Because of the extreme decrease of the calculated ice crystal phasefunctions between 0° and 1°, which can amount to five orders of magnitude, the number of expansion coefficients needed for a good fit of the phasefunctions is much too high for any practical purposes. In case of the largest crystal used in the database COP (*Hess and Wiegner, 1994*), 3000 coefficients did not yield a useful result. For this reason, a delta approximation is used before the expansion is started for all ice crystal phasefunctions.

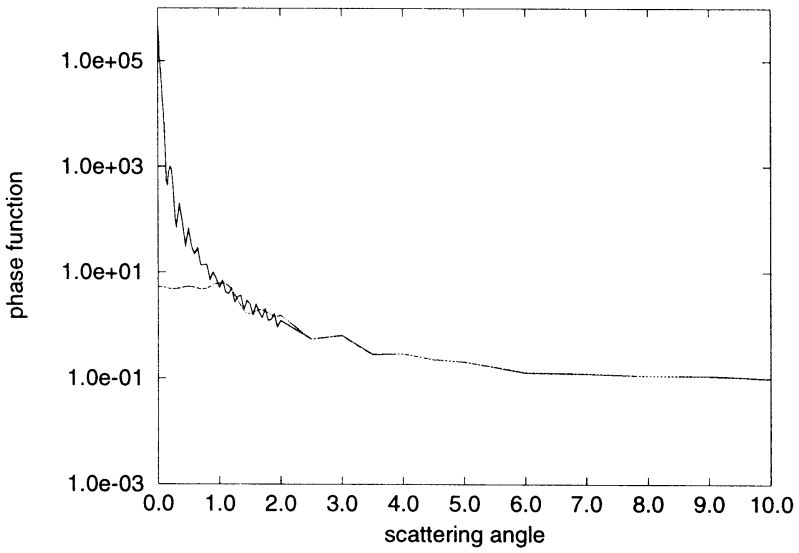

Figure 26: *δ approximation for a large hexagonal column with size 110 μm / 1300 μm at a wavelength of 0.535 μm. The dashed curve shows the approximated phasefunction reconstructed from 750 expansion coefficients.*

This delta approximation consists in cutting the forward scattering peak at a certain scattering angle θ_c. Doing so, the energy which is scattered in the near forward direction, is considered to be not scattered at all. Therefore, the scattering coefficient is reduced and consequently also the extinction coefficient and the single scattering albedo are changed. The phasefunction has to be renormalized. The cutting of the phasefunction is done in such a manner, that all phasefunction values at smaller angles are set to the value at the cut off angle. The same is done for the other diagonal matrix elements. The other elements are left unchanged. The relative amount of energy which is cut off, can be written as:

$$\delta = \int_o^{\theta_c} p(\theta) d\Omega - p(\theta_c) \int_o^{\theta_c} d\Omega \tag{28}$$

where the phasefunction $p(\theta)$ is equal to the F_{11} element. The scattering and extinction coefficients

now reduce to

$$\sigma_s' = \sigma_s \cdot (1 - \delta) \tag{29}$$

$$\sigma_e' = \sigma_e \cdot (1 - \delta\omega_o) \tag{30}$$

The new single scattering albedo is now:

$$\omega_o' = \omega_o \cdot \frac{1 - \delta}{1 - \delta\omega_o} \tag{31}$$

and the phasefunction, together with the whole scattering matrix, is renormalized by

$$p'(\theta, \phi) = \frac{1}{1 - \delta} \cdot p(\theta, \phi) \tag{32}$$

This procedure also changes the asymmetry parameter g:

$$g' = \frac{g - \delta}{1 - \delta} \tag{33}$$

An example is shown in Fig. 26. The original phasefunction of a large hexagonal column (110 / 1300 μm) is cut off at 1°. The curve shown in this figure is the approximated phasefunction after it was reconstructed from a polynomial with 750 coefficients.

Even by use of the delta approximation, the number of polynomials needed for an exact representation of the phasefunction is rather high. An objective criterion for the maximum number of polynomials needed, is the convergence of the series of coefficients. As the coefficients are monotonously decreasing and become smaller than, for example, 10^{-4}, this is a good criterion to stop the series. In case of the ice crystal phasefunctions, however, a fixed number of 750 coefficients is used, which was checked by eye to yield sufficiently good fits of all matrix elements. Nevertheless, the backscattering is not matched very well in most cases, except for the phasefunction itself. This condition is accepted to keep the calculation time of the DAK model within justifiable limits.

As cutoff angle, generally 1° is used. This value is not much different from the sun's angular dimension (0.5°), which is usually not taken into account in multiple scattering calculations. Therefore, the delta approximation introduces an acceptable limitation of the modelling of scattering properties of ice crystals (cf. also measurements of the direct sun, where often a field of view of 5° is used).

7.2 Examples

In Fig. 27 it is shown to what extent the scattering matrix elements can be described by 750 expansion coefficients and by use of a δ approximation at 1°. It can be observed that the phasefunction is represented quite well over the whole range of scattering angles, while the other matrix elements still show significant deviations in the backscattering direction. Nevertheless, these deviations are thought not to affect the multiple scattering calculations seriously. This statement should be verified however. In any case, the fit of the reconstructed scattering matrix should be checked before using the expansion coefficients. In single cases, it may happen that the representation is quite poor. In this case, a larger number of expansion coefficients should be used.

Because the raytracing code always uses the same number of coefficients (750) and the same cutoff angle in the delta approximation (1°), which may not be appropriate in all cases, there also exists a separate code to allow calculating expansion coefficients with different number of coefficients and cut off angle from existing scattering matrix calculations. This code MATEX uses the same subroutine for the expansion coefficients as the raytracing code.

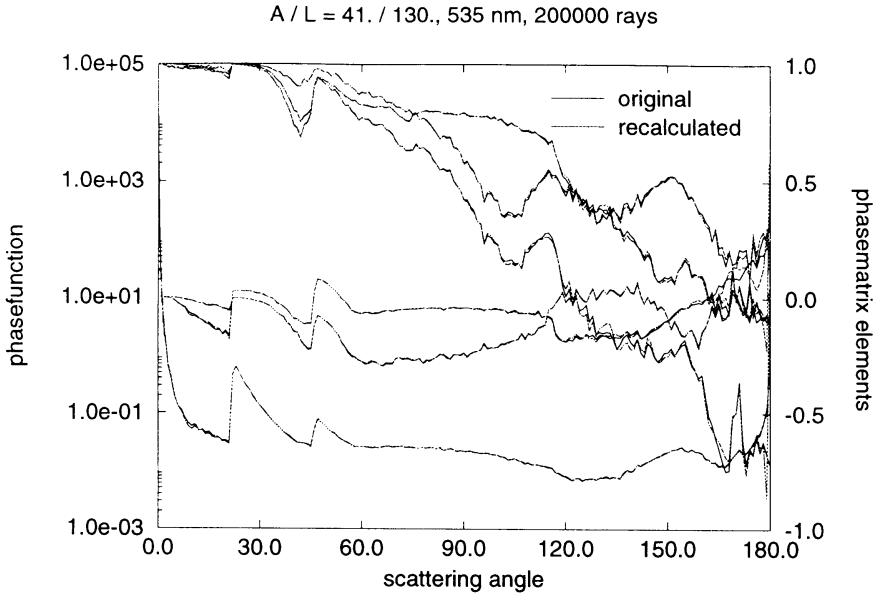

Figure 27: *original and recalculated phasefunction and scattering matrix elements for a column with size 41 μm / 130 μm at a wavelength of 0.535 μm.*

8 Testing scattering matrices

The scattering matrices which result from the raytracing code are tested using the method described in *Hovenier and van der Mee (1996)*. This method examines whether a certain 4×4 matrix can be a scattering matrix or not. Therefore, it is only a necessary condition, but it is certainly useful to detect principal errors or statistical errors in the raytracing procedure.

To perform this test, a special Fortran program has been written, because the program provided by the group of *Hovenier* is written for *Mathematica*, which is not available at KNMI. Moreover, the Fortran version allows the test to be performed automatically after the raytracing procedure. There is now also a stand alone version of the test program. The new program has been tested to reproduce the examples given in *Hovenier and van der Mee (1996)* and in the manual for the *Mathematica* program *(Schreurs, 1996)*.

In the test, the eigenvalues are determined of the so called *coherency matrix*, which is a 4×4 matrix created from the elements of the scattering matrix. The scattering matrix can only be a scattering matrix of an ensemble of particles if all eigenvalues of the coherency matrix are positive. If some eigenvalues are negative, the distance to the nearest matrix which can be a scattering matrix can be calculated from the eigenvalues with help of the *Froebenius norm*. It is also possible to create this "nearest" scattering matrix and thus correct for statistical errors in measurements or calculations.

The test is performed before the expansion of the scattering matrix in generalized spherical functions is done. The 4×4 matrix for each scattering angle is checked. If one of the matrices cannot be a scattering matrix, the nearest matrix that can be a scattering matrix is calculated by use of an optimisation procedure, and this new matrix is used instead of the original matrix in the expansion program. The relative distance between the original and corrected matrix is given as *Froebenius distance* and stored together with the corrected matrix. In all cases which have been examined up to now the relative distance between the original and corrected matrices was smaller than 10^{-4}. In most cases the correction had to be applied at forward scattering angles.

9 Application to ATSR data

In order to get an idea about the applicability of the created ice crystal scattering matrices, an attempt was made to do multiple scattering calculations with the aim to fit some ATSR-2 measurements of cirrus clouds which have been provided by *Phil Watts (pers. comm.)*.

ATSR-2 is able to measure the same cloud under two different viewing angles. Therefore, it is possible to use these measurements as a check for modelled ice crystal phasefunctions.

The ATSR-2 data consist of a number of pixels belonging to two ATSR-2 images, showing the same cirrus cloud under different viewing angles. All pixels belonging to one image have approximately the same viewing geometry. Fig. 28 shows all the data for two wavelengths (0.87 μm and 1.6 μm), together with some model calculations. The different values of the calculated radiances correspond to different cloud optical depths. The images have been taken on September, 6 1996 at 14° latitude and 134° longitude over the Pacific Ocean.

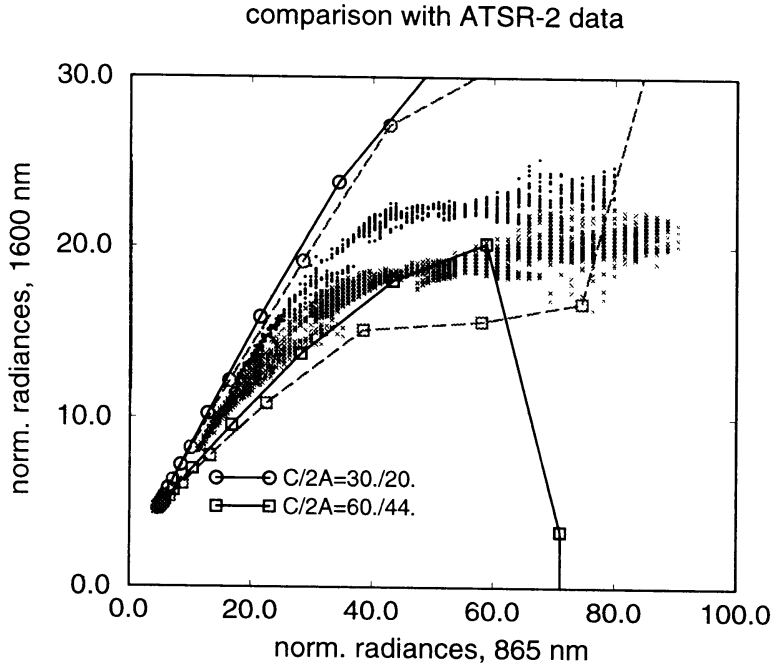

Figure 28: *ATSR-2 data at two wavelengths and two viewing angles, together with DAK model calculations for an atmosphere with cirrus clouds consisting of hexagonal columns of two different sizes. The data for nadir view are marked with circles and those for forward view with crosses. The calculations for nadir view are shown with solid lines and those for forward view with dashed lines.*

The two viewing directions correspond to scattering angles of 161° (forward view) and 121° (nadir view). The calculations have been performed with the DAK model using a standard mid-latitude summer atmosphere with a cirrus cloud at 8 km height. The optical depth is varied in 15 steps from 0 to 512 One ice crystal size has been used to model the scattering function of the cloud in each of two cases. In the first case, a hexagonal column with a dimension of 30 μm / 20 μm has been chosen and in the second case one with a dimension of 60 μm / 44 μm. The solid lines correspond to the forward view and the dashed lines to the nadir view. In both cases the maximum tilt angle was 30°. Especially for the larger particle, the DAK model produced apparently wrong results at high optical depths. The reason for this behaviour is not clear yet, but the problems will probably be due to a poor representation of the phasefunction by the expansion coefficients. Nevertheless, there is evidence from this figure, that a cloud consisting of crystals with a mean size between the two used monodisperse

cases, would satisfactorily fit the measurements. The fact that the slope of both particles does not fit all of the measurements, is easily explained by the existence of different size distributions in different parts of the image. In this case, higher optical depths would correspond to larger particle sizes.

Users' Manual for the ice crystal raytracing program SPEX

A Introduction to spex

SPEX is a ray tracing program for the calculation of the single scattering properties of ice crystals, including the complete 4×4 scattering matrix. As shapes of the ice crystals, regular hexagonal columns and plates may be used as well as spheres. In addition, it is possible to introduce a certain surface roughness, which leads to a statistical variation of the ray paths inside the crystal.

The original version of the program was made available by Peter Wendling and is described in *Wendling et al. (1979)*. It was extended by Bernhard Strauss with the possibility to do calculations for horizontally oriented particles (*Strauss, 1989*). A further extended version, which also contains absorption, diffraction at hexagonal cross sections and polarization of the scattered radiation is described in *Hess and Wiegner (1994)*. The present version additionally calculates the complete scattering matrix and also allows spheres and roughened particles as additional particle shapes.

The single scattering properties of the ice crystals consist of two independently determined parts, the raytracing part and the diffraction part. The raytracing part is calculated with help of the laws of geometric optics and the diffraction part with help of the Fraunhofer diffraction theory. Both parts are stored separately as well as added to the total scattering properties of the particle.

B How to run spex

The program needs three input files and produces quite a number of output files. The contents of all these files and the places where they are stored are described in the following subsections.

Fig. 29 shows the directory tree of `spex`. All executables and also the source code files are stored in the main `spex` directory.

B.1 Starting the program

`spex` is started by simply typing the command

```
>spex
```

This will cause the program to ask for the name of the main input file:

```
> Please enter name of inputfile without extension .inp (max.  10 char.)
As default spex.inp is used
```

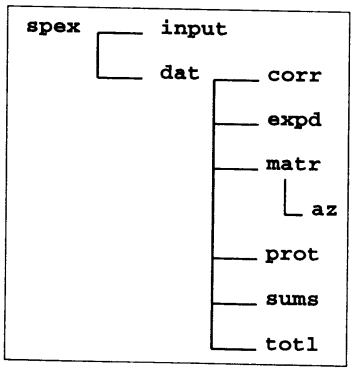

Figure 29: *Directory tree for the raytracing and related programs.*

```
################################################################################
# Input data file for SPEX
# ------------------------
#
# This file is valid for the program SPEX in the version 1.0 of
# 04.02.97. For further information see file README.
#
# INPUT DATA:#####################################################################
45.           # sun elevation angle (only used for horizontal orientation)
1.4           # A-axes of the crystal (center-edge), or radius of sphere
3.5           # C-axes of the crystal, distance from end to end (microns)
1.6           # wavelength, microns
0.            # refractive index, real part (0. = read from file)
-0.000        # refractive index, imag. part (0. = read from file)
1000000       # number of rays
no            # use convergence test?: yes, no
0.01          # convergence criterion
100000        # number of rays until next convergence test takes place
0.0           # max. angle for variation of ray direction
COLM          # crystal shape: COLM or PLAT or SPHR
RAUM          # crystal orientation: RAUM, EBEN or FEST
MIT           # calculate diffraction?: MIT, OHNE oder NUR
# END ############################################################################
```

Figure 30: Main input file for ray tracing program **spex**

Now you should enter this name, for instance:

```
test
```

(or just hit the Enter key), which will be answered by something like

```
Inputfile test.inp used
```

From now on you can leave **spex** alone for a considerable amount of time.

The given name of the input file (`test` in this example) will be used as name for the different output files, which differ in the extension to this name and in the directory where they are stored. Thus, you can easily use shell scripts for multiple calculations by including lines like

```
echo test | spex
```

with different input file names to these scripts.

B.1.1 The main input file `test.inp`

These input files are stored in the subdirectory `input`. An example of an input file is shown in Fig. 30. The meaning of the input parameters is explained in the following.

- **sun elevation angle (only used for horizontal orientation)**

  If the ice crystals are oriented randomly in a horizontal plane (of course, this option is useless for spheres), the scattering matrix as well as all the other single scattering parameters depend on the angle, under which the incoming radiation hits this plane. The scattering matrix becomes dependent on the scattering azimuth angle. The solar elevation angle has to be given in degree.

- **A-axes of the crystal (center-edge), or radius of sphere**

  Half-length of the A axis of the hexagonal crystal, or length of a side of the regular hexagon. In case of spheres, the radius has to be given. The value has to be given in μm.

- **C-axes of the crystal, distance from end to end (microns)**

  This is the length of the hexagonal column or the thickness of a plate. In case of spheres, this value is not used. The value has to be given in μm.

- **wavelength, microns**

  Wavelength of the incoming radiation in μm.

- **refractive index, real part (0 = read from file)**

  The refractive indices for ice after *Warren (1984)* are stored in the file `ice.bdt` (cf. B.1.3). If you give a 0 here, the refractive index (real and imaginary part) is read from this file. If it is not tabulated for the selected wavelength, it will be linearly interpolated between the tabulated values. If you give a value different from 0, this value will be used for the calculation.

- **refractive index, imag. part**

  If the given real part of the refractive index has not been 0, you can give here a value for the imaginary part, which will be used in the calculation. The imaginary part of the refractive index must be negative!

- **number of rays**

  The more rays you use for the ray tracing, the more accurate is the result. But the accuracy does not increase linearly with the number of rays. For particles in random orientation, you should at least use 200,000 rays, better 1,000,000. For horizontally oriented particles, it should be even more, because the angular bins for sampling of the scattered rays become smaller.

- **use convergence test?: yes, no**

  If you use the convergence test, the program stops, when the desired convergence is reached, or when the above given maximum number of rays has been used. If you do not use the convergence test, always the maximum number of rays is used.

- **convergence criterion**

  After a certain number of rays, which has to be given in the following item, the phasefunction is calculated and compared to the last realisation of the phasefunction. If the relative difference between these two phasefunctions is, in each angular bin, less than the value given here, the program stops. A convergence criterion of 0.01 will lead to at least 2 – 3 million rays.

- **number of rays until next convergence test takes place**

  This number must be large enough to yield a rather reasonable phasefunction after one single realisation. At least 50000 or 100000 should be used here.

- **max. angle for variation of ray direction**

  This is the maximum tilt angle for statistical variations of the directions of refracted and reflected rays. Values between 0° and 90° are possible. A value of 1° is suggested for nearly ideal ice crystals (only the direct forward and backward directions are affected) and 30° should be used if phasefunctions without halos are desired.

```
##############################################################################
# Configuration file for SPEX
# --------------------------
#
# This file is valid for the program SPEXin the version 1.0 of
# 09.12.96. For further information see file README.
#
# !! DO NOT CHANGE THIS FILE UNLESS YOU REALLY KNOW WHAT YOU ARE DOING !!
#
# INPUT DATA :#################################################################
1             # number of runs using same input data
99            # number of considered Wechselwirkungen (99=unlimited)
1.E-04        # termination condition for each ray
1             # toggle test of unit vectors (1=on)
0             # toggle conversion of Stokes vector (0=on, 1=off, 2=off,unnormalized)
1             # toggle use of rotation matrix (0=off)
NAT           # polarisation of incident radiation: NAT, LIN, HORZ,VERT
no            # choose different field of angles
3             # number of intervals with equidistant angular bins
0.            # first angle
2.            # last angle
0.5           # increment
3.            # first angle
178.          # last angle
2.            # increment
178.5         # first angle
180.          # last angle
0.5           # increment
# END ########################################################################
```

Figure 31: Configuration file for ray tracing program **spex**

- **crystal shape: COLM or PLAT or SPHR**

  As crystal shapes, hexagonal columns (COLM), hexagonal plates (PLAT) or spheres (SPHR) are possible. For columns $C/2A > 1$ and for plates $C/2A < 1$. If you enter the wrong crystal type here (for instance COLM for a particles with $C/2A < 1$), the program will stop.

- **crystal orientation: RAUM, EBEN or FEST**

  Columns and plates may be oriented randomly in space (RAUM), randomly in a horizontal plane (EBEN), or they may be fixed relative to the direction of the incoming radiation (FEST). In case of random orientation in space, all directions of incidence of the incoming radiation relative to the crystal occur with equal probability. In case of horizontal orientation, these possible directions of incoming radiation are restricted according to the geometrical conditions for the given sun elevation angle. Fixed orientation is only possible for pure diffraction calculations. For spheres, this choice has no influence.

- **calculate diffraction?: MIT, OHNE oder NUR**

  You can do raytracing calculations together with diffraction calculations (MIT), without diffraction (OHNE), or you can calculate diffraction without raytracing calculations (NUR).

B.1.2 The configuration file `spex.cfg`

This file is stored in the main **spex** directory. This file should never be changed, unless you are very sure about what you are doing. It is mainly meant to give possibilities for test runs. Do not forget to reset changed values after your tests have been performed. The default values are shown in Fig. 31.

- **number of runs using same input data**

There is a loop over the whole raytracing part of the program. It can be used to get several runs with identical input parameters, but different random numbers. This possibility has never been tested with the new program versions, and probably will not work any more.

- **number of considered Wechselwirkungen (99=unlimited)**

  You can limit the maximum number of interactions a ray can have with crystal faces. If you do not limit the number of interactions, the ray is traced until its weight becomes smaller than the termination condition given below. The meaning of possible values is:

  - 0: only externally reflected rays
  - 1: + transmitted rays (halos)
  - 2: + 1 internal reflection
  - 3: + 2 internal reflections
  - ...
  - 99: no limitation

- **termination condition for each ray**

  Each ray starts the raytracing with a weight of 1. During the ray tracing, the ray is split several times and absorption takes place. Thus, the weight becomes smaller. This value determines, at what size of the ray the tracing of this ray is stopped.

  `1.E-04` seems to be very useful.

- **toggle test of unit vectors (1=on)**

  This produces a lot of output in the protocol file `dat/prot/test.pro` if there are unit vectors, which are for some reasons not unity. If this happens, something went wrong with an attempted change in the program.

- **toggle conversion of Stokes vector (0=on, 1=off, 2=off,unnormalized)**

  The program uses the Stokes vector in the form $[I_\perp, I_\parallel, U, V]$. This is changed to $[I, Q, U, V]$ before the results are stored. At the moment it is not clear what happens if this option is turned off.

- **toggle use of rotation matrix (0=off)**

  You can switch all rotations of the matrices during the ray tracing off. It is not recommended to turn this off.

- **polarisation of incident radiation: NAT, LIN, HORZ, VERT**

  This choice is obsolete. Always use NAT!

- **choose different array of angles**

  This option allows a change of the default angular grid for the ray tracing. These angles are the boundaries of the angular bins where the scattered rays are sampled. The scattering angles of the scattering matrix will be the centres of these intervals. It is not possible to use an array of scattering angles larger than the default number of 183. The default array of scattering angles consists of an equally spaced array with 1° distance and additionally with a small angular bin in the direct forward and backward directions.

- **number of intervals with equidistant angular bins**

  This and the following lines are only read if you decided to change the field of scattering angles. You can use as many intervals with equidistant angular bins as you like. For each of these intervals, you must give in the following lines the begin (`first angle`) and the end (`last angle`) of the interval and the increment (`increment`), which shall be used between the lower and upper limits of this interval.

B.1.3 The refractive index file `ice.bdt`

The file `ice.bdt` contains the refractive indices for ice as they are given in *Warren (1984)*. The table has been completely transferred for wavelengths between 0.195 μm and 10 μm and contains in addition some values which have been linearly interpolated between the original values. They are marked by **. At wavelengths larger than 10 μm only certain values exist, which have been needed for special purposes. Since the raytracing program interpolates linearly between the values tabulated in `ice.bdt`, one should be careful with wavelengths larger than 10 μm. The imaginary part of the refractive index must be given negative for use in the raytracing program.

B.2 The output files

The raytracing program and the connected programs produce a large number of output files. The contents of these files will be described in the following. The filenames consist of the name of the input file, extended by a certain extension and they are stored in different subdirectories. These subdirectories must exist before the program is run.

- `dat/prot/test.pro`

  These files contain error messages and other informations describing the program run. There are also some results and control values given.

- `dat/totl/test.bg`

  Here, the results belonging to the old version, without scatteringmatrix, are stored. This also includes the diffraction function and the pure raytracing phasefunction, given for the angular field used in the raytracing.

- `dat/matr/`

  In this directory the matrix results of the raytracing are stored.

  - `test.md`

    This is the complete 4×4 scattering matrix with the diffraction part added. In addition, the most important input data and the other single scattering data as the extinction coefficient or the asymmetry parameter are given.

  - `test.ma`

    Here, the diffraction is not added, and the matrix is given at the angles used in the raytracing program.

- `dat/matr/az/test.p11 ... dat/matr/az/test.p44`

  This directory contains the scattering matrices of horizontally oriented particles. There is 1 file for each of the 16 matrix elements. The first column in each file contains the scattering angles and the following columns contain the corresponding scattering matrix values at all the scattering azimuth angles.

- `dat/expd/`

  This directory contains all results related to the expansion coefficients, which are calculated from the scattering matrix for use in the radiative transfer code DAK. They are calculated after the raytracing procedure is finished and always use 750 coefficients and a cut off angle of 1° for the δ approximation. It is possible to change these default values by use of the program `matex`.

  - `test.dak` can be used as input for DAK.
  - `test.out` contains additional informations about the expansion, including all input data used.
  - `test.rec` contains the scattering matrix elements, which have been calculated from the expansion coefficients. This can be used as a (subjective) check for the quality of the expansion.

- `dat/corr/test.cs`

  This directory contains output of the scattering matrix test and correction program after *Hovenier and van der Mee (1996)*. The matrix test is running before the expansion coefficients are calculated. The expansion coefficients are calculated from the corrected matrix. The program `matest` may also be started separately to perform scattering matrix tests. The files `*.cs` contain the 6 corrected scattering matrix elements for randomly oriented particles. For each angle is indicated whether the matrix had to be corrected or not and how large the relative distance between the original and the corrected matrix is.

- `dat/sums/`

  This directory is not used by the ray tracing program but contains all the output files created by the program `coma` which does a size distribution averaging over ray tracing results. The files here are of the same type as in the `dat/expd/` directory and there is a `test.ms` file which contains the scattering matrix of the sum of particles of different sizes.

C The source code

The program is written in Fortran. It compiles well with `f77` (warning errors about common block misalignment may be ignored) on a SGI O2 workstation, but used also to be happy with `f90`. All real variables are double precision. The complete code is divided in several files, each containing a number of subroutines and functions. The whole stuff is most easily compiled with help of the `spex/Makefile`. All Fortran files are stored in the `spex` directory. The contents of all the different files is roughly described in the following sections.

C.1 `spex.f`

This file contains the raytracing part of the program. It consists of the following parts:

- `program spex`

  The main program starts all the necessary subroutines, but also includes some calculations, for example the selection of the point where the ray enters the crystal, or the calculation of the scattering matrix after the raytracing is done. There is also still a lot of obsolete code which is no longer used and should be removed one day.

- `subroutine flac`

  This subroutine defines the geometry of the particle itself and relative to the direction of the incoming ray.

- `subroutine richtg`

  Here the directions of the reflected and refracted rays and their energy according to Fresnel's formulas are calculated.

- `subroutine drucken`

  Drucken is german for to print. Most of the output of the program is produced here.

- `subroutine strik`

  This is the main raytracing part of the program (**Str**ahl **i**m **K**ristall). The intersections of rays with the crystal are determined, the necessary rotations of the scattering matrix are performed and absorption along the ray path is calculated.

- `entry straus in subroutine strik`

  Here the rays that leave the crystal are sampled and put in their appropriate angular bins.

- `subroutine stasum`

  Sums energy in angular bins for convergence test.

- `subroutine statest`

  Performs convergence test.

- `subroutine chan`

  Calculates directions of tilted plane normals and the new angles of incidence needed for the calculation of reflected and refracted directions and of the Fresnel formulae.

- `subroutine binary`

  This is needed to determine the number of the angular bin for a ray leaving the crystal under a certain scattering angle. It makes use of the logical functions `ltheta` and `lchi`.

C.2 `beugung.f`

This file contains all the subroutines for calculating diffraction:

- `subroutine beugung`

  Here the calculation of diffraction is organized. In case of hexagonal crystals, the subroutine `bghexe` is called for fixed orientations of the crystal relative to the incoming radiation, and the integration over a number of orientations is performed. An angular increment of 5^o is used for the orientation averaging.

  In case of spheres, the subroutine `disp` is called.

- `subroutine bghexe`

  `bghexe` calculates the diffraction pattern of a hexagonal particle in fixed orientation after *Takano and Asano (1983).*

- `subroutine disp`

  This one calculates the diffraction for a sphere and does integration over the size distribution ($n(r) = n_o r^6 e^{(-9r/R)}$) around the size of the sphere.

C.3 `pollibd.f`

This is a collection of several numerical subroutines, which are not directly connected to the ray tracing program.

- `function ran3`
  is a random number generator from numerical recipes.
- `subroutine zufall`
  is used to activate the random number generator. Always the same seeding value is used!
- `subroutine zuzahl`
  creates a new random number.
- `subroutine trapez`
  performs linear interpolations.
- `subroutine traplo`
  also performs linear interpolation, but the logarithm of the ordinate values (y-axis) is used.
- `subroutine gerin`
  is a routine for trapez integration.
- `subroutine theta18n`
  defines the angular field for the diffraction part.
- `subroutine chik`
  defines the scattering azimuth angles in the diffraction program.
- `subroutine chibt3`
  is also used by the diffraction program.

C.4 `libd.f`

This file contains several linear algebra routines from `linpack` and `lapack`, and some of the necessary `blas` routines. These routines are freely available on the web from *NAG Ltd.* (address: http://www.netlib.org/lapack), but are also installed as precompiled libraries on many systems. There is also one matrix multiplication routine from the `SSP` (scientific subroutine package) included. All these routines are not listed here.

C.5 `expandf.f`

This consists of the original Piet-Stammes-`expand.f`-routine for calculating the expansion coefficients from phasefunctions. The reading procedure of the phasefunctions has been modified a little bit for the purposes of ice crystal scattering. There is also a new `subroutine deltap` which does a delta-approximation on the ice crystal phasefunctions.

C.6 `scatest.f`

This subroutine performs a test on the scattering matrix after *Hovenier and van der Mee (1996)*. If the tested matrix seems to be no scattering matrix, it also applies a "correction formalism" which produces a new matrix which can be a scattering matrix, and shows the relative distance to the original matrix.

C.7 cheev.f

This are lapack routines needed for the calculation of eigenvectors and eigenvalues. They are used by the scattering matrix test programs.

C.8 blaslib.f

These blas routines are needed for the cheev program.

D Additional programs

There are 3 additional programs, which can be run after the ray tracing has been done, and which use the output of the ray tracing program as input. matex and matest do the same as corresponding subroutines which are run directly after the ray tracing (in fact, they use the same subroutines). They can be used to change the results of the expansion and of the matrix test. coma is used to calculate single scattering of mixtures of ice crystals.

D.1 matex: calculate expansion coefficients

This program reads an output file of spex or coma, calculates the expansion coefficients, and stores the results in 3 files in the directory dat/expd or dat/sums respectively.

When you start the program with the command matex, you are asked for the following:

```
Type of phasefunction:
(1) single crystal
(2) size distribution
```

"single crystal" means that a result of spex is used (dat/matr/test.md), while "size distribution" uses a result of the program coma (dat/sums/test.ms).

The next question askes for the name of the data file. Here, you must omit as well the file path as the file extension:

```
Give name of scattering matrix file (<=20 chars.)  >
```

Now, the number of expansion coefficients has to be entered, which you want to consider. Note, that the DAK model cannot handle more than 750 coefficients, which is also the default used by the ray tracing program:

```
Give number of coefficients (<=10000) >
```

The last question is about the scattering angle, at which the phasefunction shall be cut for the delta-approximation:

```
cutting angle for delta-approximation:
```

1° is used as default in the ray tracing program.

The results of this program run will overwrite any former results.

D.2 matest: test and correct scattering matrices

This program reads an output file of spex or coma, performs a test on the scattering matrices at all angles, eventually calculates a "corrected" matrix, and stores the results in a file in the directory dat/corr. For test and "correction", the method described in *Hovenier and van der Mee (1996)* is applied.

The program will ask the following questions:

```
Type of phasefunction:
(1) single crystal
(2) size distribution
(3) pure ray tracing (single crystal)
```

"single crystal" means that a result of spex is used (dat/matr/test.md), while "size distribution" uses a result of the program coma (dat/sums/test.ms). "pure ray tracing (single crystal)" means a ray tracing result without diffraction added (dat/matr/test.ma).

Now, you are asked for the name of the result file containing the matrix you want to test. You must omit the file path and the file extension:

```
Give name of scattering matrix file (<=20 chars.)  >
```

The results of this program are written on files like dat/corr/test.cs. Former results will be overwritten.

D.3 coma: calculate scattering properties for size distributions

This program uses results of the ray tracing program for particles of different sizes to calculate size distribution weighted averages of the single scattering properties. All needed ray tracing calculations have to be performed before coma is started. coma relies on certain conventions about the number of size intervals and the sizes of the particles (see Table 1). For each calculation of size distribution weighted scattering properties, the scattering matrices of the 8 columns or 6 plates must exist for the desired wavelength. There is also a convention about the composition of the names of the files in dat/matr/ which shall be used as input files in coma (the files *.md are used). These file names must have the following form:

```
c40550r30
```

- c:

  The first letter indicates the particles shape. Available shapes are:

  - c: columns
  - p: plates

- 4:

  The number gives the size of the particle. The intervals are numbered in the following way: b a 1 2 3 4 5 6. b is the smallest and 6 the largest particle. The sizes belonging to these intervals are shown in Table 1.

```
# database contents available for program COMA
#
# 1. wavelengths
#
# the wavelengths must be given with 4 digits, describing the
# wavelength in nm. They are read in A-format.
#
6                              # number of wavelengths (max. 33)
0535                           # wavelengths
0550
0659
0865
1600
3700
#
# 2. tilt angles
#
# the tilt angles must be given with 2 digits, describing the
# maximum tilt angle. They are read in A-format.
3                              # number of max. tilt angles (max. 10)
00                             # tilt angles
01
30
```

Figure 32: Configuration file `coma.cfg` for program `coma`.

- 0535:

  These numbers are the wavelength. 4 digits must be used. The example corresponds to 0.535 μm. All wavelengths for which a complete set of calculations (at least all 8 or 6 sizes for one particle shape) exists, must be given in the configuration file `coma.cfg` in the main `spex` directory. An example of this file is shown in Fig. 32.

- `r`:

  indicates random orientation.

- 30:

  This is the maximum tilt angle used in the ray tracing calculations. It must be given with 2 letters. A maximum tilt angle of 1° would read "`01`". The possible tilt angles must be given in the configuration file `coma.cfg`.

Once started, the program asks several questions. First, the desired wavelength must be given. Here, the wavelengths are shown for selection, which the program found in `coma.cfg`:

```
please select wavelength:
(1) 0535 nm
(2) 0550 nm
(3) 0659 nm
(4) 0865 nm
(5) 1600 nm
(6) 3700 nm
```

The next question is about the tilt angle:

```
please select tilt angle:
```

```
(1) 00
(2) 01
(3) 30
```

Now, the desired type of size distribution must be given:

```
please decide which kind of size distribution you want to use:
(1) Heymsfield and Platt (1984)
(2) Liou (1989)
(3) own number densities
(4) read number densities from file "numin"
```

- `Heymsfield and Platt (1984)` Here, one of 8 temperature dependent size distributions may be selected (the temperatures are in °C):

  ```
  please select size distribution:
  (1):  -20 to -25
  (2):  -25 to -30
  (3):  -30 to -35
  (4):  -35 to -40
  (5):  -40 to -45
  (6):  -45 to -50
  (7):  -50 to -55
  (8):  -55 to -60
  ```

  These size distributions are restricted to sizes larger than 20 μm. Thus, the size intervals `b` and `a` are not used.

- `Liou (1989)`

  This is a parametrization of the above mentioned 8 size distributions with respect to cloud temperature. The desired temperature must be given:

  ```
  please enter temperature between -20 and -60 C
  ```

- `own number densities`

  Here, you can enter interactively your own number densities for all 8 intervals.

- `read number densities from file "numin"`

  Same as above, but you enter the number densities in the file **numin**.

The next question is about the mixing ratio between columns and plates:

```
you may mix columnar and platelike crystals.
please enter mixing ratio of columns (number le.  1)
```

The results of this program are stored in the directory `dat/sums`. The last question asks for the name of the output files:

```
Please enter name of outputfile without path and extension (max.  10 char.)
```

This produces an output file, for instance `dat/sums/test.ms`. This file is then used as inputfile for the expansion coefficients program, which stores the output files `test.dak`, `test.out` and `test.rec` in the directory `dat/sums`. These are the same types of files as described above for the directory `dat/expd`. Also a file `dat/corr/test.cs` is created from the matrix test subroutine.

References

[1] Auer, H.A. and D.L. Veal (1970): *The dimensions of ice crystals in natural clouds*, J. Atm. Sci., **27**, 919–926

[2] Coulson, K.L. (1988): *Polarization and scattering of light in the atmosphere*, A. Deepak Publ., Hampton

[3] Deirmendjian, D. (1969): *Electromagnetic Scattering on Spherical Polydispersions*, American Elsevier, New York

[4] Gish, K.R. (1988): *Ray Optics Calculations of the Scattering Matrix of Clouds of Spherical and Spheroidal Particles*, M.Sc. Thesis, Free University Amsterdam

[5] de Haan, J.F., P.B. Bosma and J.W. Hovenier (1987) : *The adding method for multiple scattering calculations of polarized light*, Astron. Astrophys. **183**, 371–391

[6] Hess, M. (1996): *Modellierung und Messung optischer Eigenschaften von Cirren*, Ph.D. Thesis, Universität München

[7] Hess, M. and M. Wiegner (1994): *COP: a data library of optical properties of hexagonal ice crystals*, Appl. Opt., **33**, 7740–7746

[8] Heymsfield, A.J. and C.M.R. Platt (1984): *A Parametrization of the Particle Size Spectrum of Ice Clouds in Terms of the Ambient Temperature and the Ice Water Content*, J. Atm. Sci., **41**, 846–855

[9] Hovenier, J.W. and C.V.M. van der Mee (1996): *Testing scattering matrices: a compendium of recipes*, J. Quant. Spectrosc. Radiat. Transfer, **55**, 649–661

[10] van de Hulst, H.C. (1957): *Light scattering by small particles*, J. Wiley & Sons, New York; also Dover, New York, 1981

[11] Liou, K.N. (1992): *Radiation and Cloud Processes in the Atmosphere*, Oxford University Press, Oxford

[12] Liou, K.N. and J.E. Hansen (1971): *Intensity and Polarization for Single Scattering by Polydisperse Spheres: A Comparison of Ray Optics and Mie Theory*, J. Atm. Sci., **28**, 995–1004

[13] Macke, A., J. Mueller, and E. Raschke (1996): *Single Scattering Properties of Atmospheric Ice Crystals*, J. Atm. Sci., **53**, 2813–2825

[14] de Rooij, W.A. and C.C.A.H. van der Stap (1984): *Expansion of Mie scattering matrices in generalized spherical functions*, Astron. Astrophys., **131**, 237–248

[15] Schreurs, R. (1996): *Testing scattering matrices, using Mathematica*, M.Sc. Thesis, Free University Amsterdam

[16] Stammes, P. (1994): *Errors in UV reflectivity and albedo calculations due to neglecting polarisation*, in: Proceedings of the European Symposium on Satellite Remote Sensing, 26–30 September, 1994, Rome. EOS/SPIE volume 2311, 227–235

[17] Strauss, B. (1989): *Modellierung der Einfachstreuung an hexagonalen Eiskristallen - mit besonderer Beruecksichtigung der horizontalen Ausrichtung der Eiskristalle*, M.Sc. Thesis, Universität München

[18] Takano, Y. and S. Asano (1983): *Fraunhofer Diffraction by Ice Crystals Suspended in the Atmosphere*, J. Met. Soc. Jap., **61**, 289-300

[19] Takano, Y. and K. Jayaweera (1985): *Scattering phase matrix for hexagonal ice crystals computed from ray optics*, Appl. Opt., **24**, 3254–3263

[20] Warren, S.G. (1984): *Optical constants of ice from ultraviolet to the microwave*, Appl. Opt., **23**, 1206-1225

[21] Wendling, P., R. Wendling, and H.K. Weickmann (1979): *Scattering of solar radiation by hexagonal ice crystals*, Appl. Opt., **18**, 2663-2671